



Cite this: *Anal. Methods*, 2025, 17, 3083

## Sensing technology empowering food safety: research progress of SERS-assisted multimodal biosensing toward food hazard factors

Jiaqian Liu,<sup>†a</sup> Xiaowei Huang,<sup>†a</sup> Xinai Zhang,<sup>ID</sup> <sup>\*a</sup> Yuerong Feng,<sup>a</sup> Zhecong Yuan,<sup>a</sup> Shujie Gao,<sup>a</sup> Zhihua Li,<sup>a</sup> Hany S. El-Mesery,<sup>b</sup> Jiyong Shi,<sup>ID</sup> <sup>\*a</sup> and Xiaobo Zou,<sup>ID</sup> <sup>\*a</sup>

Food is the main source of human energy and nutrition, but once it is contaminated with hazardous factors, such as biotoxins, pesticide residues, etc., it will seriously damage health. This paper reviews the research progress of biosensors based on surface-enhanced Raman scattering (SERS) in the detection of food hazard factors. First, the basic principle, substrate and assay mode of SERS technology, as well as related design and sensing strategy mechanisms, are introduced. Then, the design idea of multimodal biosensors combining SERS with microfluidic, fluorescence, colorimetric, electrochemical (EC), molecular imprinting and other technologies is expounded to improve the analysis accuracy and specificity. Then the application results of multimodal biosensors based on SERS sensing toward food hazard factors are discussed, and the necessity of its development is illustrated. Finally, the future development direction of this field is prospected, which provides a reference for promoting the research and application of multimodal biosensors based on SERS.

Received 21st February 2025

Accepted 27th March 2025

DOI: 10.1039/d5ay00292c

rsc.li/methods

### Introduction

The presence of various harmful factors in food poses a serious threat to human health, and their rapid and accurate detection

is essential to ensure food safety.<sup>1</sup> As the primary source of energy and nutrition for sustaining life activities, food is of particular concern from a public health perspective. When consumed under safe conditions, food provides the body with

<sup>a</sup>School of Food and Biological Engineering, Jiangsu University, Zhenjiang 212013, P. R. China. E-mail: zhangxinai@ujs.edu.cn; shi\_jiyong@ujs.edu.cn; Zou\_xiaobo@ujs.edu.cn

<sup>b</sup>School of Energy and Power Engineering, Jiangsu University, Zhenjiang 212013, P. R. China

<sup>†</sup> These authors contributed equally to this work.



Jiaqian Liu

Jiaqian Liu obtained her BS in Food Science and Engineering from Jiangsu University (2024) and is pursuing her MS degree in the Non-destructive Technology and Intelligent Equipment for Agricultural Products research group at the university's School of Food Science and Engineering, supervised by Prof. Xiaobo Zou. Her research focuses on surface-enhanced Raman spectroscopy (SERS) and chiral molecular recognition, aiming to develop ultrasensitive detection methods.



Xiaobo Zou

Dr Xiaobo Zou received his PhD degree in Agricultural Product Processing and Storage Engineering from Jiangsu University (2005) and currently holds dual roles as the Vice President of the institution and Dean of its School of Food and Biological Engineering. Having held visiting professorships at the University of Leeds and Utah State University, he spearheads innovative research in non-destructive quality and safety

assessment of agricultural products, multimodal sensing technologies, odor visualization systems, and hyperspectral/near-infrared imaging applications. He serves as the Vice Chairman of the Jiangsu Institute of Food Science and holds the position of an Associate Editor for the journal *Frontiers in Food Science*.

essential nutrients such as proteins, carbohydrates, fats, vitamins, and minerals for proper functioning.<sup>2,3</sup> However, contamination of food with harmful substances can have far-reaching and serious consequences for human health.<sup>4</sup> Many food-accumulating contaminants can transfer to humans *via* the food chain, harming human health.<sup>5</sup>

Microbial contamination, for instance, has been identified as a significant hazard. Food contaminated with pathogenic *Escherichia coli* (*E. coli*), *Listeria monocytogenes* (*L. monocytogenes*), *Staphylococcus aureus* (*S. aureus*), and *Vibrio parahaemolyticus* (*V. parahaemolyticus*) can cause acute gastroenteritis, food poisoning, and even bacteremia and meningitis.<sup>6–8</sup> Chemical contaminants, such as pesticide residues,<sup>9,10</sup> veterinary drug residues, heavy metals,<sup>11–13</sup> and illegal additives<sup>14,15</sup> also pose a significant threat to public health. The long-term ingestion of food containing pesticide residues has been demonstrated to potentially disrupt the endocrine system, nervous system, and immune system of the human body.<sup>16</sup> Furthermore, the accumulation of heavy metals in the human body has been shown to interfere with the body's normal metabolism and physiological functions by impeding the body's antioxidant defense mechanisms.<sup>17</sup> Consequently, the establishment of an accurate and timely food hazard factor detection system is imperative for the management and prevention of foodborne diseases.

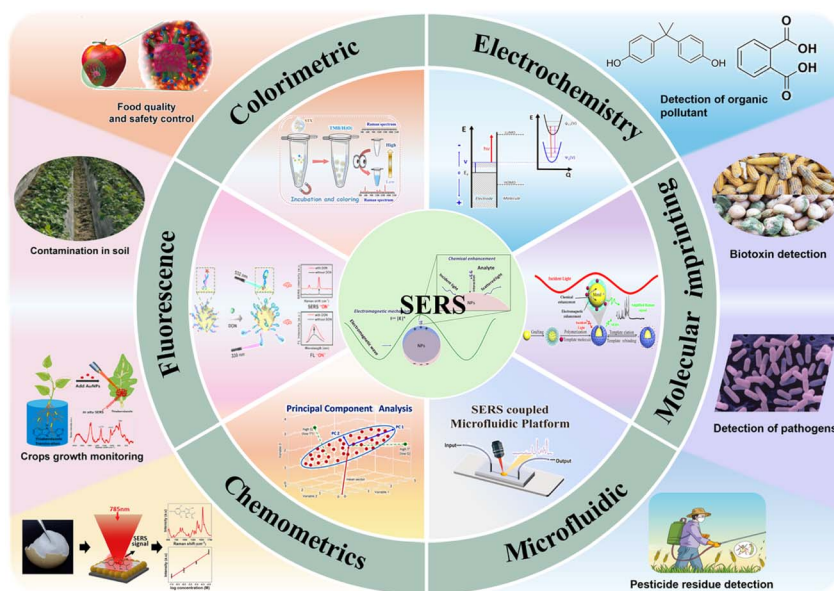
Conventional food hazard detection methodologies principally encompass chemical and instrumental analysis. Chemical analysis methodologically involves the qualitative and quantitative analysis of substances through chemical reactions, such as the titration method, which is employed to ascertain the content of acids, bases, salts, and other constituents in food.<sup>18</sup> The colorimetric method utilizes the comparison of the color shade of the solution to determine the concentration of noxious substances, such as nitrites.<sup>19</sup> These methods are characterized by simplicity in operation and cost-effectiveness. However, they are limited in terms of sensitivity and selectivity and are primarily applicable to the identification of macronutrients or semi-micronutrients. Instruments are employed in instrumental analysis methods, which utilize a range of instruments for the analysis of substances. Common spectral analysis methods, such as atomic absorption spectrometry and atomic fluorescence spectrometry, can detect the presence of heavy metals in food. Chromatography, including gas chromatography, liquid chromatography, and others, is extensively employed in the realm of pesticide residue,<sup>20–22</sup> mycotoxin,<sup>23</sup> and related compound detection. Mass spectrometry, boasting high sensitivity and resolution, facilitates precise characterization and quantification of trace hazardous substances within complex samples. This method is well-suited for expeditious analysis of a substantial number of samples and the determination of trace hazardous substances.<sup>24</sup> However, note that limitations remain due to complex sample pretreatment and high associated costs.

In recent years, there has been a proliferation of bio-analytical methods that have been developed to address the need for rapid, on-site, and cost-effective diagnostics. These methods, which are based on nucleic acid, immunology, and

biosensor technologies, have been proposed as a means of overcoming the limitations of conventional detection techniques. The integration of nanotechnology with these bio-analytical methods has the potential to enhance sensitivity and specificity, while also reducing cost and facilitating more rapid analysis.<sup>25</sup> The underlying principle of bioanalytical methods is the specific reaction of an organism to a substance, which can be used to analyze the organism in question. For instance, the enzyme-linked immunosorbent assay (ELISA) employs the specific binding reaction of an antigen with an antibody to expeditiously detect antibiotic residues, toxins, and the like in food.<sup>26–28</sup> Conversely, biosensors integrate biometric components with physical or chemical transducers to translate biological signals into quantifiable electrical or optical signals for real-time monitoring of hazardous substances.<sup>29–31</sup> Bio-analytical methods are characterized by their high specificity and sensitivity, rendering them particularly well-suited for the discernment of trace quantities of hazardous substances in complex samples. However, these methods are also accompanied by significant financial costs and a limited discernment range. Among the developed techniques, SERS has emerged as a prominent research focus due to its distinctive advantages.<sup>32–34</sup> SERS boasts several notable benefits, including ultra-high sensitivity, the capacity for fingerprinting information, and the miniaturization of equipment.<sup>35–37</sup> The exceptional sensitivity of SERS enables the detection of individual molecules, thereby making it an invaluable tool for food safety applications where contaminants may be present at trace levels.<sup>38</sup> The capacity to acquire “fingerprint” spectra of diverse substances enables the identification and quantification of contaminants in intricate food matrices.<sup>35</sup>

However, the SERS technique itself still faces some challenges, such as the need for homogeneous and reproducible substrate preparation, the sensitivity of data analysis to background interference, and the presence of false-positive results due to nonspecific binding of analytes. In order to effectively address these issues, a promising research direction is the combination of SERS assays with other techniques to construct multimodal biosensors.<sup>39</sup> In recent years, significant advancements have been made in the field of food hazard monitoring with SERS-based multimodal biosensors. Compared to traditional unimodal sensors, these multimodal sensors possess the capability to utilize multiple independent response signals for cross-validation, thereby enhancing the accuracy and reliability of the analysis.<sup>40,41</sup>

In practical applications, SERS has been integrated with colorimetric, fluorescence,<sup>42,43</sup> and molecular blotting<sup>44</sup> techniques to leverage the strengths of each method. This paper provides a comprehensive summary of the research progress of SERS-based multimodal biosensors for food hazard factors (Scheme 1). It is important to emphasize that while this review utilizes food safety as a representative application scenario, the core objective lies in exploring universal strategies to enhance the performance of SERS-based detection platforms. The methodologies discussed here, which span substrate design, signal amplification, and multimodal integration, are inherently transferable to other domains requiring ultrasensitive



Scheme 1 SERS-based detection mechanism and application of multimodal biosensing toward food safety.

molecular detection, such as biomedical diagnostics and environmental monitoring.

## SERS sensing principle toward food safety testing

### SERS sensing principle

The principle of Raman spectroscopy is based on the Raman scattering effect. When a beam of monochromatic light, such as a laser, strikes a substance, most of the photons are scattered at the same frequency, which is Rayleigh scattering. However, a small number of photons interact with the vibrational patterns of molecules in the substance, causing the frequency of the photons to change. When a molecule jumps from the ground state to the vibrational energy level of the excited state, the photons lose energy and the frequency decreases, resulting in Stokes scattering. If the molecule is already in a vibrationally excited state, the photons can absorb the vibrational energy, increasing the frequency and causing anti-Stokes scattering.<sup>45</sup>

SERS uses electromagnetic radiation and scattering between materials to analyze the structural information of the target and relies on a metal substrate with a rough surface to enhance the Raman signal of the molecules. It is fast, simple, and non-destructive and requires no sample pretreatment.<sup>46</sup> Usually gold, silver and copper are common SERS substrates for effectively enhancing Raman signals. The widely recognized SERS signal enhancement mechanism has two aspects. One is the physical enhancement process, that is, the electromagnetic enhancement effect caused by the excitation of local surface plasma motifs.<sup>47,48</sup> The second is the chemical enhancement process, that is, the charge transfer enhancement effect caused by the change of the polarizability of molecules adsorbed on the rough metal surface.<sup>39</sup> These two signal enhancement models are both related to the behavior of the tested molecules on the

SERS substrate. Therefore, the SERS-based biosensor can respond rapidly and extremely sensitively to molecular adsorption, transformation, and interaction, greatly enhancing detection sensitivity (Fig. 1).

### SERS substrate design

SERS substrates are mainly divided into colloidal substrates and solid substrates. Colloidal SERS substrates composed of Au or Ag nanogels have negative or positive charges on their surfaces due to the action of organic ligands.<sup>49</sup> However, the same electrostatic force could prevent molecules with similar charges from absorbing on the colloid surface, and the distance between the molecules and the active surface of SERS increases, resulting in the weakening of the SERS signal.<sup>50</sup> Solid SERS substrates fix metal nanoparticles on a solid surface.<sup>51</sup> Although it is difficult to design and manufacture, it is favored for its stability and durability. When preparing high-performance SERS substrates, the size, shape, composition, and particle spacing of nanomaterials are key parameters that need to be controlled and optimized.<sup>52</sup> These factors affect the strength of "hot spots".<sup>53,54</sup> With the development of nanotechnology, different nanomaterials such as nanorods, nanowires, nanospheres, and nanosheets have emerged, each of which has unique enhancement properties.<sup>55</sup> Digital (nano)colloid-enhanced Raman spectroscopy is likely to be the top choice for reliably and ultra-sensitively detecting various analytes (Table 1).<sup>56</sup>

Novel SERS substrates exhibit multifaceted advantages over traditional substrates. In terms of enhancement performance, porous nanosheets, core-shell nanocomposites, and similar materials can generate stronger SERS enhancement effects by designing and optimizing the size, morphology, and structure of nanomaterials, thereby improving detection sensitivity.<sup>57,58</sup> For example, modifying the morphology of gold to create sharp

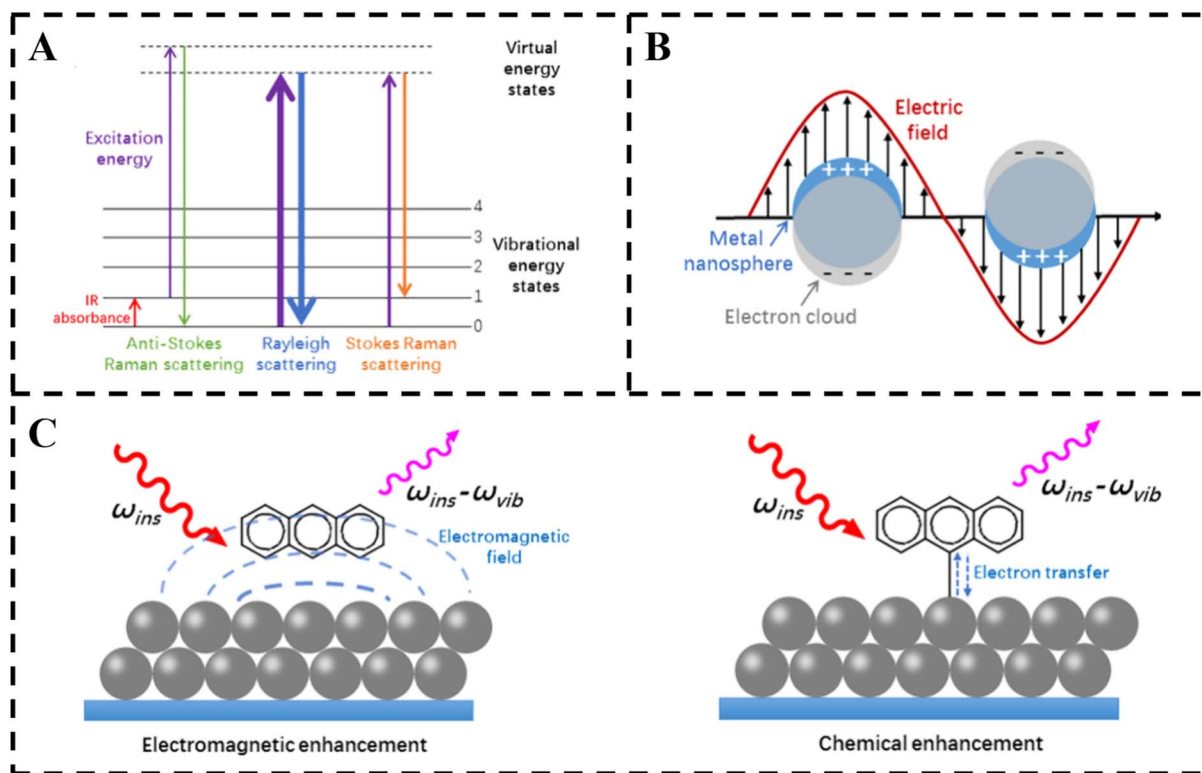


Fig. 1 (A) The energy level diagram for Raman scattering. (B) Schematic illustrations of the excitation of localized surface plasmon resonance (LSPR). (C) Schematic illustration of electromagnetic (left) and chemical enhancement (right) of Raman scattering signals of a molecule adsorbed on the surface of noble metal nanoparticles.<sup>35</sup>

tips and rough surfaces, or leveraging the “hotspot” effects from nanogaps and tips of noble metals, can significantly enhance Raman signals.<sup>59</sup> Simultaneously, combining electromagnetic enhancement (EM) and chemical enhancement (CM) mechanisms, such as utilizing strong interfacial coupling and efficient charge carrier separation in semiconductor heterojunctions, greatly improves the utilization efficiency of photoinduced electrons in the substrate, enabling efficient charge transfer in the substrate–molecule system and thus significantly enhancing SERS performance.<sup>60,61</sup>

In terms of uniformity and reproducibility, improving the reproducibility of SERS substrates is one of the key challenges in practical applications. This can generally be achieved by optimizing nanoparticle synthesis and deposition methods, refining substrate fabrication processes, and incorporating internal standards (ISs). In terms of nanoparticle synthesis and deposition, techniques such as photolithography, nano-imprinting, or template-assisted self-assembly can be used to fabricate ordered nanostructures (*e.g.*, nanopore arrays) with precise control over nanoparticle size, shape, and spacing, thereby creating uniformly distributed hotspots.<sup>62,63</sup> Studies have shown that synthesizing Au/metal or non-metal oxide heterostructured nanoparticles and then uniformly depositing them onto a substrate can induce strong plasmonic coupling at the Au/oxide interface, achieving high-sensitivity SERS analysis with excellent signal reproducibility.<sup>64</sup> In substrate fabrication process improvement, Lafuente *et al.*<sup>65</sup> employed Langmuir–

Schaefer technology to prepare uniform SERS substrates in a reproducible and straightforward manner. Celik *et al.*<sup>66</sup> reported a facile method for the non-lithographic fabrication of plasmonic nanoparticle arrays by utilizing the barrier sides of anodized aluminum oxide (AAO) membranes. Finally, incorporating internal standards into SERS substrates can effectively enhance the reproducibility of Raman signals. For example, based on a systematic evaluation of competitive adsorption between ISs and target analytes, Lin *et al.*<sup>67</sup> applied the proposed pressure drop-coating (PDC) method to fabricate an IS-modified gold nanobipyramids (Au NBPs)/anodic aluminum oxide (AAO) SERS substrate within 1 minute, demonstrating high reproducibility of Raman signals.

In terms of functionalization and multi-scenario applicability, the development of magnetic and flexible substrates can support rapid separation, enrichment, and detection of curved surface samples.<sup>68,69</sup> Designing temperature-sensitive or pH-sensitive polymer-modified substrates enables dynamic regulation of SERS activity.<sup>70</sup> In recent years, researchers have conducted extensive studies on flexible SERS substrates, successfully preparing various high-performance flexible SERS substrates using polydimethylsiloxane (PDMS), filter paper (FP), biofilms, textiles, and metal meshes as supporting materials.<sup>71–75</sup> Although flexible SERS substrates exhibit excellent performance in adapting to irregular surfaces and portable detection, they still have certain limitations compared to rigid substrates. Issues such as nanoparticle detachment, stress–

Table 1 Common SERS substrates and characteristics

Substrate type	Representative materials	Characteristics
Colloidal substrates	Gold nanoparticles (AuNPs)	Simple to prepare and have a good SERS-enhancement effect, but have poor selectivity, reproducibility and stability Have good plasmonic activity in the entire visible to near-infrared region and can provide a relatively strong SERS-enhancement effect, but have relatively poor chemical stability and are prone to oxidation in air Have a certain SERS-enhancement ability, but have poor chemical stability and may corrode in some application environments Good stability and excellent biocompatibility
	Silver nanoparticles (AgNPs)	
	Copper nanoparticles (CuNPs)	
	Composite noble metal nanomaterials (such as Au@Ag, Ag@Au, and Au@Pt) Magnetic nanomaterials (such as Fe <sub>3</sub> O <sub>4</sub> /Ag, Fe <sub>3</sub> O <sub>4</sub> @Au, Ni/Au, and Ni/Ag)	
Solid substrates	Semiconductor composite materials (such as Ag/TiO <sub>2</sub> , Ag/ZnO, Ag/CuO, and Si/Au) Graphene nanocomposites (such as CNTs/Ag NPs and GO/Ag)	The use of magnetism can realize the detection, separation and enrichment of the analyte, improve the sensitivity of SERS detection and simplify the pre-treatment of complex samples SERS chemical enhancement and photoelectric catalytic properties Large surface area, good optical properties, easy to functionalize, good electrical conductivity and low fluorescence background signal
	Noble metal nanomaterials (such as Au, Ag, and Cu)	The preparation process is relatively mature, have high stability and can provide a reliable enhancement signal, but are not applicable to the detection of samples with irregular shapes and surfaces
	Semiconductor nanocomposites (such as TiO <sub>2</sub> substrates)	Have SERS chemical enhancement and photoelectric catalytic properties, but the preparation process is relatively complex and the stability is relatively poor
	Magnetic nanocomposites (such as Fe <sub>3</sub> O <sub>4</sub> /Ag and Fe <sub>3</sub> O <sub>4</sub> @Au)	The use of magnetism can realize the detection, separation and enrichment of the analyte, improve the sensitivity of SERS detection and simplify the pre-treatment of complex samples, but the preparation process is relatively complex and the stability is relatively poor

induced deformation, polymer fluorescence interference, and surface roughness significantly reduce the mechanical stability and signal-to-noise ratio of flexible substrates.<sup>76</sup> In recent years, many researchers have attempted to address these shortcomings. For example, Hu *et al.*<sup>77</sup> proposed a novel process of femtosecond laser nanoparticle array (NPA) implantation to address the issue of nanoparticle stability on flexible substrates. Additionally, the differences in thermal expansion coefficients and insufficient chemical tolerance of flexible substrates limit their application in extreme environments. Rigid substrates, on the other hand, remain dominant due to their high mechanical stability, corrosion resistance, relatively mature fabrication processes, and lower technical difficulty. Therefore, although flexible substrates have potential in specific scenarios, rigid substrates remain the mainstream choice for high-sensitivity and high-reproducibility requirements. Future research could explore “rigid-flexible composite” strategies to balance stability and deformation adaptability.

In terms of detection sensitivity and selectivity, leveraging the  $\pi$ - $\pi$  interactions of two-dimensional materials such as graphene to adsorb aromatic molecules can enhance molecular enrichment capabilities and lower detection limits.<sup>78</sup> Substrate modification with antibodies or aptamers enables targeted molecular capture, such as for the specific recognition of cancer biomarkers (Table 2).<sup>79,80</sup>

From the above discussion, it is evident that significant progress has been made in research, but substrate design inherently requires trade-offs between performance metrics. Colloidal substrates, although cost-effective and suitable for solution environments, are limited by their random hotspot distribution and finite shelf life due to nanoparticle aggregation or oxidation. Solid-state ordered arrays exhibit high reproducibility but rely on expensive fabrication techniques and rigid substrates, limiting their application in flexible environments. Core-shell structures improve stability, but if the shell thickness exceeds the optimal limit, it may weaken the electromagnetic field, while complex synthesis processes affect batch consistency. Flexible substrates enable conformal detection on irregular surfaces but still face challenges such as nanoparticle detachment and thermal/chemical instability. Magnetic composites are recyclable but suffer from non-uniform hotspot distribution due to magnetic aggregation and interfacial strain caused by mismatched thermal expansion coefficients. However, studies have been dedicated to addressing these issues. For example, Chen *et al.*<sup>81</sup> developed a surfactant-free method to stabilize colloidal cit-AuNPs based on alkali regulation, and this method can prevent gold nanoparticle aggregation under different harsh treatments, including ligand modification, centrifugation-based washing/enrichment, and salt addition. Zhang *et al.*<sup>82</sup> developed a highly dispersible gold

Table 2 Types and specific examples of traditional and novel SERS substrates

Category	Type	Specific examples
Traditional SERS substrates	Rough metal electrodes	Roughened silver (Ag), gold (Au), and copper (Cu) electrodes
	Metal colloidal nanoparticles	Gold and silver nanoparticle colloids prepared by chemical reduction, forming randomly aggregated “hot spots”
	Metal films and island structures	Rough metal films prepared by vacuum evaporation or sputtering, forming nanoscale metal island structures
New SERS substrates	Disordered nanostructures	Etched metal surfaces or randomly distributed metal nanoparticles, relying on statistical hot spot distribution
	Ordered nanostructure arrays	Nanorod/nanowire arrays ( <i>e.g.</i> , Au nanorods prepared using AAO templates) Nanopore arrays ( <i>e.g.</i> , anodic aluminum oxide templates combined with metal deposition)
	Composite structure materials	Periodic nanostructures fabricated by lithography or electron beam etching ( <i>e.g.</i> , nanopillars and nanocube arrays) Core-shell structures ( <i>e.g.</i> , Au@SiO <sub>2</sub> and Ag@TiO <sub>2</sub> , combining stability and enhancement capabilities) Metal-semiconductor heterojunctions ( <i>e.g.</i> , Au-TiO <sub>2</sub> and Ag-ZnO, utilizing synergistic enhancement effects) Magnetic composite materials ( <i>e.g.</i> , Fe <sub>3</sub> O <sub>4</sub> @Au, enabling easy separation and recycling)
	Two-dimensional material substrates	Graphene/graphene oxide (GO) combined with metal nanoparticles, enhancing chemical adsorption and electron transfer Transition metal dichalcogenides ( <i>e.g.</i> , MoS <sub>2</sub> and WS <sub>2</sub> ) combined with metal nanostructures
	Flexible substrates	Polymer-coated metal nanostructures ( <i>e.g.</i> , PDMS and PET) Paper-based or textile substrates, suitable for irregular surface detection
	Single-particle/single-molecule substrates	Tip-enhanced structures ( <i>e.g.</i> , atomic force microscopy tips modified with metal nanoparticles) Metasurfaces designed with plasmonic resonance structures

nanorod (GNR) powder using an octadecyl trimethylammonium bromide (C<sub>18</sub>TAB)-assisted freeze-drying method to form a sponge-like crystal structure. This method effectively inhibits the aggregation of GNRs during the drying process, overcoming the bottleneck of traditional colloidal storage instability.

Currently, high-performance ordered arrays remain economically unfeasible for large-scale deployment, and substrates that simultaneously optimize sensitivity, stability, and stimulus responsiveness are rare. The lack of standardized characterization protocols further hinders comparisons across different studies. Future research must prioritize scalable nanofabrication techniques and AI-driven design to address the complex parameter space. By tackling these challenges, SERS technology will transcend laboratory limitations and enable transformative applications in biomedical diagnostics, environmental monitoring, and industrial sensing.

#### Effects of different substrate preparation strategies on the properties of SERS and application challenges in the food industry

In the system of flexible substrates, plasmonic nanoparticles, and analytes, different substrate preparation strategies significantly influence the chemical interactions among the three, thereby affecting SERS performance. Physical methods, due to high temperature and energy, may cause oxidation or

deformation of flexible substrates, reducing surface functional groups and increasing hydrophobicity, leading to weak binding between nanoparticles and substrates with low chemical activity. Analytes primarily bind to nanoparticles through non-specific adsorption. Cheng *et al.*<sup>83</sup> deposited Au-Ag nanoparticle arrays on PDMS substrates treated with atmospheric plasma *via* sputtering, finding that plasma treatment increases active groups on the PDMS surface, thereby enhancing nanoparticle adhesion, improving the binding mode between the substrate and nanoparticles, and boosting SERS detection performance. Gao *et al.*<sup>84</sup> prepared silver nanoparticles on flexible substrates using evaporation for ultrasensitive explosive detection. The results showed that the high-temperature evaporation process may cause slight oxidation or deformation of the substrate, affecting the binding strength between the nanoparticles and the substrate, thereby influencing SERS signal stability.

Chemical methods require pretreatment of flexible substrates to introduce active groups, which may reduce flexibility, but nanoparticles can firmly bind to the substrate *via* chemical bonds, and their surfaces can be modified with ligands. Analytes achieve specific binding through ligand mediation, but steric hindrance may reduce adsorption efficiency. Wang *et al.*<sup>85</sup> prepared gold nanoparticle arrays on PDMS substrates *via* chemical reduction and encapsulated them with

a ternary film, forming a stable, flexible, and high-performance SERS chip. This preparation method enables specific capture of analytes, significantly improving detection sensitivity and selectivity.

Self-assembly methods require highly uniform surfaces on flexible substrates, which may limit their applicability, but they enable ordered nanoparticle arrangement, enhancing plasmonic coupling effects. Additionally, high-density functional groups can promote directional adsorption of analytes but may hinder the diffusion of large molecules. Bian *et al.*<sup>86</sup> coated silver nanoparticles on cotton fabric using molecular self-assembly technology, creating an ultrasensitive and flexible SERS substrate. The ordered self-assembly of nanoparticles on cotton fibers not only enhanced plasmonic effects but also provided high-density active sites for analyte adsorption and detection. These chemical interactions directly determine the system's signal sensitivity, flexibility compatibility, detection limits, and selectivity. For example, chemical bonding offers higher long-term stability than physical adsorption, nanoparticle surface modification improves the specific capture efficiency of analytes, substrate treatment requires balancing functionalization and mechanical properties, non-specific adsorption leads to high background noise, and directional modification enhances the signal-to-noise ratio (Table 3).

Although SERS substrates demonstrate high sensitivity and rapid detection advantages in laboratory settings, they still face multiple challenges when applied in the food industry. For example, various molecules in food matrices may compete for the active sites on SERS substrates, reducing the adsorption efficiency of target analytes. Additionally, some SERS substrates (*e.g.*, colloidal nanoparticles) are prone to aggregation or oxidation in complex solutions, leading to signal fluctuations and compromising detection reliability. From a cost perspective, high-performance SERS substrates rely on expensive technologies, making it difficult to meet the large-scale detection demands of the food industry. While flexible substrates are suitable for detecting irregular food surfaces, issues such as nanoparticle detachment require additional optimization costs. Practical food samples often require complex extraction and purification steps to remove interferents, diminishing the rapid screening advantage of SERS. Existing technologies, such as immunochromatographic test strips, hold greater advantages in rapid screening scenarios. Despite these challenges, the potential of SERS substrates in the food industry remains promising. In the future, functionalized designs, such as core-shell structures to enhance stability and intelligent algorithm-

assisted analysis, are expected to drive breakthroughs in the application of SERS substrates in specific scenarios.

## SERS assay modes toward food safety testing

As illustrated in Fig. 2, the detection of SERS technology can be divided into two categories: direct detection (label-free detection method) and indirect detection (labeled detection method).<sup>87</sup> The two detection methods have their own advantages and disadvantages.

### Label-free SERS assay

Label-free SERS assay is a simple analytical method, which generally uses precious metal colloids and nanostructured metal surfaces as substrates.<sup>35,88</sup> The fundamental mechanism is predicated on the direct interaction of precious metal nanostructures with target molecules, thereby generating specific fingerprint signals. This method takes advantage of the inherent Raman scattering properties of molecules near plasma active surfaces.<sup>89</sup>

Several research teams have optimized the local electromagnetic field enhancement and molecular adsorption efficiency through substrate design in various dimensions. For example, Lin *et al.*<sup>90</sup> developed a three-dimensional gold nanobipyramid-anodic aluminum oxide (Au NBP-AAO) composite substrate, where the ordered nanogaps form dense "hotspots" that directly capture aflatoxin B<sub>1</sub> in peanut extracts and generate characteristic peaks (Fig. 3A). Zheng *et al.*<sup>91</sup> constructed a graphene oxide-gold nanofilm (GO@Au-Au), leveraging the large specific surface area of two-dimensional materials and the synergistic effect of gold nanostructures to achieve simultaneous identification of multiple mycotoxins (Fig. 3B). Chakraborty *et al.*<sup>92</sup> loaded silver nanoparticles onto the surface of reduced graphene oxide, enhancing the capture of Raman signals from pesticide residues through charge transfer at the metal-carbon interface (Fig. 3C). Meanwhile, Chen *et al.*<sup>93</sup> proposed a three-dimensional fiber filter paper substrate, establishing a scalable three-dimensional hotspot array by uniformly distributing a monolayer of gold nanoparticles within the cellulose network (Fig. 3D). The commonality among these studies lies in their use of noble metal nanounits as the core for electromagnetic field enhancement. By designing the macroscopic structure of the substrate, such as three-dimensional porosity, two-dimensional films, and fiber

**Table 3** Key differences in chemical interactions between different substrate preparation strategies

Preparation strategy	Substrate-particle interaction	Particle-analyte interaction	Typical application scenarios
Physical methods	Weak (physical adsorption)	Primarily non-specific adsorption	Low-cost rapid fabrication, short-term detection
Chemical methods	Strong (covalent/coordination bonds)	High specificity (requires functionalization)	Biosensing, high-sensitivity detection
Self-assembly methods	Moderate (intermolecular forces)	High-density directional adsorption	High-precision molecular recognition

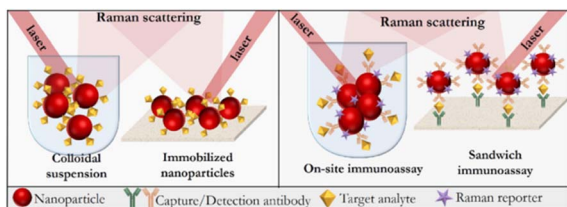


Fig. 2 Schematic representation of the direct and indirect approaches for SERS-based detection.<sup>87</sup>

networks, the density of active sites is increased. The introduction of heterogeneous materials, such as AAO and GO, improves the dispersion and stability of nanoparticles. This synergistic structure-material innovation strategy provides a universal design approach for label-free SERS detection.

However, label-free SERS detection in complex food matrices is still challenging because other molecules with similar chemical structures may interfere.<sup>94</sup>

### Labeled SERS detection

Unlike the direct detection method, the indirect detection method collects not the information of the test object itself, but the molecular vibration information of the SERS tag<sup>95</sup> (Fig. 4). A typical SERS tag used in the field of biological analysis includes four parts: substrate, Raman probe molecule, protective shell and identification molecule. Based on SERS, biometric elements (such as antibodies, aptamers, molecularly imprinted

polymers, *etc.*) are introduced. These biometric elements can specifically identify target biomolecules (such as proteins, nucleic acids, pathogens, *etc.*). When the target biomolecules are bound to the biometric elements, they will be fixed on the surface of metal nanostructures. Due to the surface-enhanced Raman effect, the Raman signal of the target molecule is significantly enhanced. By obtaining these characteristic Raman signals, qualitative and quantitative analysis of the target biomolecules can be realized. This technique is useful for identifying and quantifying targets in complex sample matrices.<sup>96</sup>

For example, Wu *et al.*<sup>97</sup> utilized 1,2-bis(4-pyridyl) ethylene molecules to bridge AuNPs into dimer probes, achieving indirect detection through signal attenuation caused by the binding of aptamers to aflatoxin B<sub>1</sub> (AFB<sub>1</sub>). She *et al.*<sup>98</sup> modified AuNPs with monoclonal antibodies and 4-mercaptopbenzoic acid (MBA) to construct an immunochromatographic-SERS dual-mode probe for ultrasensitive detection of mercury ions in water. Chen *et al.*<sup>99</sup> and Li *et al.*<sup>100</sup> designed dual-functional magnetic nanoprobe (Fe<sub>3</sub>O<sub>4</sub>@Au capture probe/Au@Ag reporter probe) and molecularly imprinted-SERS composite substrates (SiO<sub>2</sub>@TiO<sub>2</sub>@Ag@MIPs), respectively, enhancing detection specificity through aptamer competition or selective adsorption by imprinted cavities, with the latter also exhibiting self-cleaning functionality.

In pathogen detection, Duan *et al.*<sup>101</sup> and Li *et al.*<sup>102</sup> employed sandwich-type SERS probes (*e.g.*, Au@Ag core-shell nanoparticle-aptamer complexes) or competitive signal amplification strategies based on GNR aggregation, achieving rapid



Fig. 3 (A) Schematic diagram of preparation of the Au NBP-AAO SERS substrate.<sup>90</sup> (B) Preparation of a thin film GO@Au-Au SERS nano-label and design schematic of a SERS ICA test strip based on GO@Au-Au.<sup>91</sup> (C) Diagrammatic representation of detection of thiram residue in apple/tomato peel using SERS.<sup>92</sup> (D) FOS modification of the filter paper enables direct formation of sputtered Au NPs for hot spot engineering, along with a hydrophobic condensation effect for analyte manipulation, dramatically enhancing the Raman signals.<sup>93</sup>



Fig. 4 General steps and design criteria in engineering of SERS tags for biomedical applications.<sup>95</sup>

identification of Salmonella and staphylococcal enterotoxins, respectively (Fig. 5A and B). Chattopadhyay *et al.*<sup>103</sup> and Duan *et al.*<sup>104</sup> further introduced magnetic nanoparticles (FPMNPs, SiO<sub>2</sub>@Au) as capture substrates, combined with surface antibody or aptamer modifications, to enrich target bacteria through magnetic separation and reduce background interference (Fig. 5C and D).

Wu *et al.*<sup>105</sup> and Duan *et al.*<sup>106</sup> developed test strips and PDMS membrane substrates, utilizing aptamer competition principles or dual-probe sandwich structures to achieve on-site rapid detection of zearalenone (ZEN) and multiple pathogens, highlighting the application potential of portable devices (Fig. 6A and B). To address complex matrix interference, Sun *et al.*<sup>107</sup> constructed a nitrile-mediated competitive immunosensor,



Fig. 5 (A) Schematic illustration of a SERS-based aptasensor for quantification of *S. typhimurium*.<sup>101</sup> (B) Schematic illustration of this proposed SERS-based aptasensor for *S. typhimurium*.<sup>102</sup> (C) (i) Modification of synthesized GNPs with MBA and DSNB; (ii) synthesis of FPMNPs and bio-conjugation with CSA-1-Ab; (iii) magnetically assisted capture of *S. typhimurium* and its detection using the SERS signal probe.<sup>103</sup> (D) Schematic illustration of a SERS-based aptasensor for *V. parahaemolyticus* detection using SiO<sub>2</sub>@Au core/shell NPs as the substrate.<sup>104</sup>

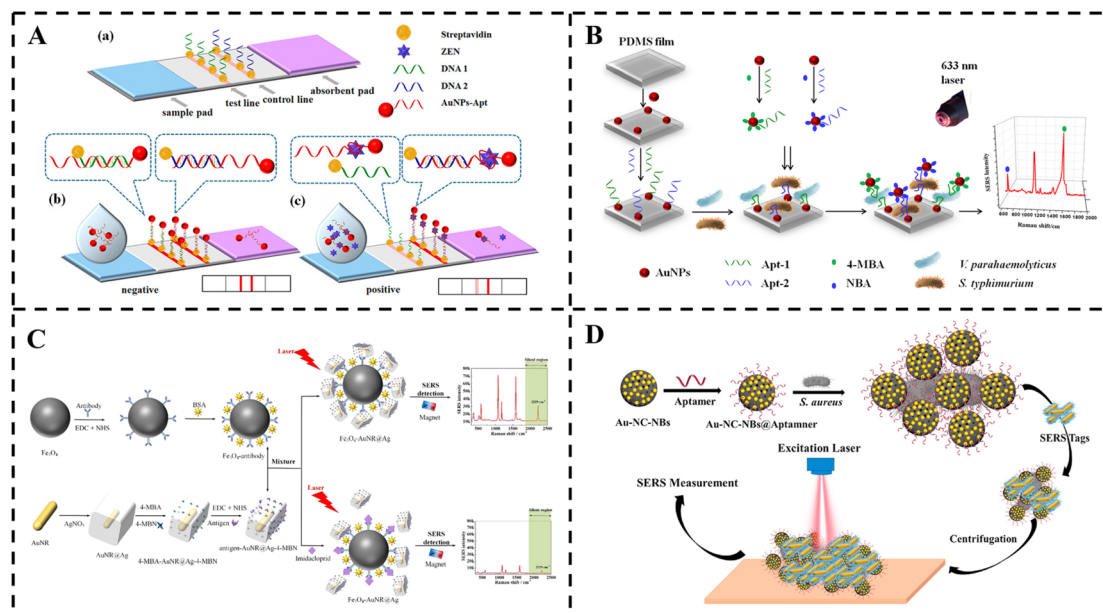


Fig. 6 (A) Aptamer-based lateral flow test strip.<sup>105</sup> Structure of the test strip (a). Negative test: in the absence of ZEN (b). Positive test: in the presence of ZEN (c). (B) Schematic representation of a SERS aptasensor for simultaneous detection of multiple pathogens utilizing an Au-PDMS film as the active substrate.<sup>106</sup> (C) Scheme showing the competitive immunoassay detection procedures.<sup>107</sup> (D) A new template-induced strategy for the controlled synthesis of hollow and porous Au-NC nanoballoons with excellent performance for the detection of bacteria both in testing samples and real samples via surface-enhanced Raman scattering assay.<sup>108</sup>

while Xie *et al.*<sup>108</sup> enhanced aptamer loading capacity using nitrogen-doped porous gold nanorods (Au-NC-NBs), improving the anti-interference capability for pesticide and *S. aureus* detection, respectively (Fig. 6C and D).

Weng *et al.*<sup>109</sup> and Ma *et al.*<sup>110</sup> designed fully functional nanosensors integrating magnetic enrichment and ratiometric SERS detection or gold/silver heterodimer probes, enabling high-throughput analysis of *E. coli* and mixed pathogens (Fig. 7A and B). Zhu *et al.*<sup>111,112</sup> innovatively combined  $\text{Fe}_3\text{O}_4$ @Au@Ag nanocomposites with gold foil paper, achieving ultrasensitive detection of multiple pathogenic bacteria through a negative correlation response induced by probe dissociation (Fig. 7C and D).

From the above discussion, it is evident that these studies widely employ core-shell structures, magnetic composites, or heterointerfaces to enhance local electromagnetic fields and chemical stability. Simultaneously, selectivity is improved through aptamer/antibody directional modification, molecular imprinting, or competitive binding mechanisms. Alternatively, magnetic separation, test strips, or flexible substrates are used to simplify pretreatment steps. Compared to label-free SERS, labeled strategies offer advantages such as strong specificity, outstanding anti-matrix interference capability, and improved quantitative accuracy through signal amplification or ratiometric detection. However, their limitations include high probe synthesis complexity, longer detection times in some systems, and potential reproducibility issues due to photobleaching of signal molecules. These challenges may be partially mitigated or even complemented by the synergistic integration of SERS with other technologies.

## SERS-based multimodal biosensing toward food safety testing

### SERS-based chemometrics

The complexity of SERS data often necessitates the use of chemometric techniques for effective analysis. Chemometrics involves the application of statistical and mathematical methods to extract meaningful information from complex datasets.<sup>113</sup> In the context of SERS, chemometric techniques can enhance the interpretation of spectral data and facilitate the identification of unknown compounds. Recent studies have demonstrated the effectiveness of various chemometric methods, such as Partial Least Squares (PLS), Principal Component Analysis (PCA), and Competitive Adaptive Reweighted Sampling (CARS), in the analysis of SERS spectra. Data obtained from label-free SERS detection are sometimes combined with certain chemometric models for analysis to enhance the accuracy of detection. Guo *et al.*<sup>114</sup> explored the potential of combining chemometrics and multivariate analysis with SERS, as well as the exploration of novel SERS substrate platforms. Wang *et al.*<sup>115</sup> pointed out that the combination of SERS with chemometric algorithms is of significant importance for ensuring food safety, emphasizing the role of multiple regression models in food monitoring.

In recent years, the integration of SERS with chemometrics has demonstrated significant advantages in food detection, with researchers achieving precise analysis and classification of target analytes through various strategies. These studies generally adopt a framework of spectral preprocessing and multivariate model optimization to address issues such as noise

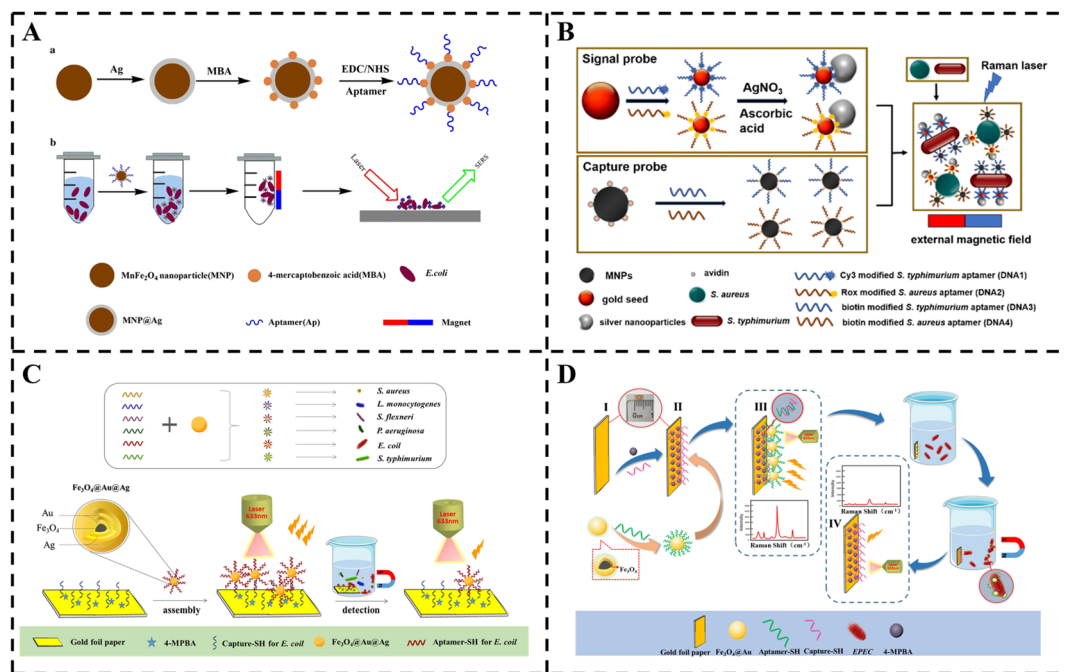


Fig. 7 (A) Schematic diagrams of the preparation (a) and application (b) of the all-in-one magnetic SERS nanosensor for *E. coli* detection.<sup>109</sup> (B) Schematic illustration of the developed gold/silver nanodimer SERS probes to detect *S. typhimurium* and *S. aureus* simultaneously.<sup>110</sup> (C) Schematic diagram of the aptasensor assembly and detection of pathogenic bacteria.<sup>111</sup> (D) Schematic illustration for EPEC detection with SERS analysis and magnetic separation technology.<sup>112</sup>

interference, signal overlap, and complex matrix effects in SERS data. For example, Hassan *et al.*<sup>34</sup> and Zhu *et al.*<sup>116</sup> employed preprocessing methods such as wavenumber selection, second

derivatives, and mean centering (MC) to eliminate baseline drift, combined with variable selection algorithms or projection dimensionality reduction techniques, significantly enhancing

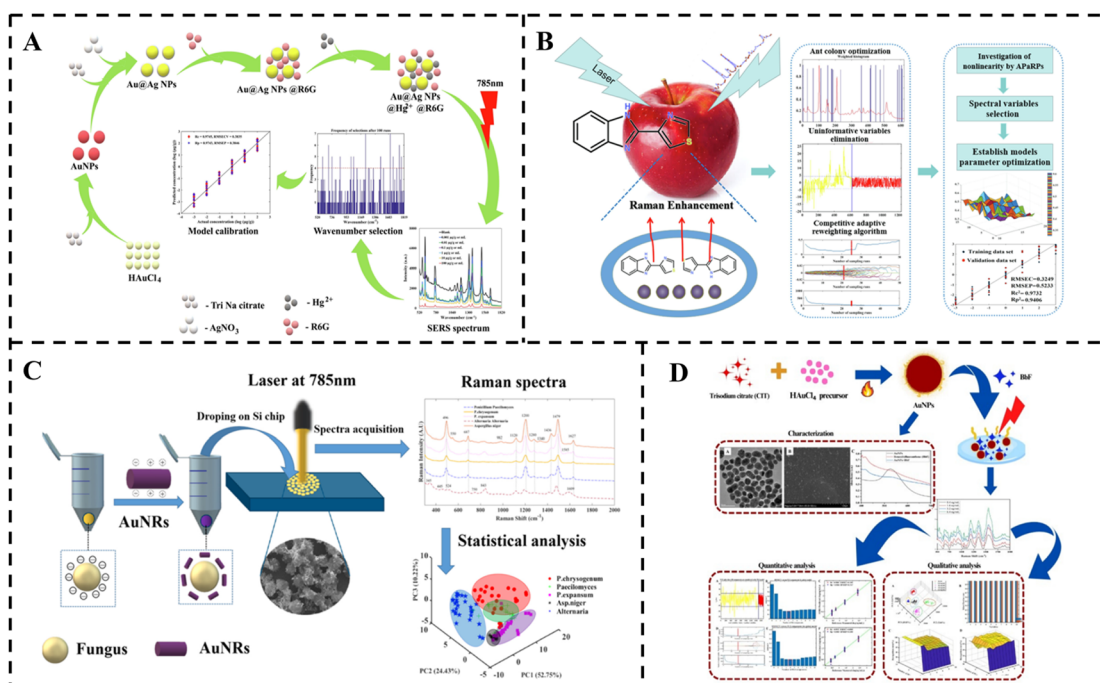


Fig. 8 (A) Outline of the sensing mechanism involved in the prediction of  $Hg^{2+}$  in fish and water samples.<sup>34</sup> (B) Schematic description of this proposed method to determine thiabendazole residue in apple using SERS coupled with ACO-ELM, UVE-ELM and CARS-ELM comparatively.<sup>117</sup> (C) Schematic illustration of the SERS measurements on fungus using gold nanorods.<sup>118</sup> (D) Schematic illustration of fabrication of the SERS substrate and detection of BbF.<sup>120</sup>

the model's ability to identify low-concentration targets (Fig. 8A). Among them, Li *et al.*<sup>117</sup> and Guo *et al.*<sup>118</sup> further addressed the limitations of traditional linear methods in complex nonlinear relationships by introducing nonlinear models (*e.g.*, CARS-ELM and BPANN), highlighting the importance of chemometric model adaptability (Fig. 8B and C).

Additionally, some studies emphasize the enabling role of chemometrics in the practical application of SERS technology. Firstly, through the process of preprocessing-feature extraction-model optimization, raw spectral information is transformed into interpretable chemical fingerprints. Secondly, Liu *et al.*<sup>119</sup> and Adade *et al.*<sup>120</sup> leveraged the complementarity of supervised and unsupervised learning to simultaneously achieve the dual goals of quantitative detection and qualitative identification (Fig. 8D). Finally, Jiang *et al.*<sup>121</sup> and Guo *et al.*<sup>122</sup> enhanced model robustness by algorithm-driven variable screening (*e.g.*, Bootstrap Soft Shrinkage, BOSS) to reduce dimensionality (Fig. 9A).

However, many current studies still primarily focus on laboratory-simulated samples. For instance, the studies by Jiao *et al.*,<sup>123</sup> Zeng *et al.*,<sup>124</sup> and Guo *et al.*<sup>125</sup> require further exploration of the interference mechanisms of multi-component coexistence in real food matrices (Fig. 9B–D). In the study by Li *et al.*,<sup>117</sup> the evaluation of the advantages and disadvantages of CARS-ELM and siPLS-ACO lacks a unified algorithmic assessment standard. Furthermore, the impact of nano-substrate stability and spectral reproducibility on model generalization capability has not been systematically quantified.

It is noteworthy that several studies have attempted to break through traditional paradigms. For instance, Hassan *et al.*<sup>34</sup>

established a rapid screening model for mercury ions by combining wavenumber selection with the signal response mechanism of SERS probes, demonstrating the role of chemometrics in optimizing signal utilization within specific wavelength intervals. Guo *et al.*<sup>122</sup> designed an aptamer-regulated nanoparticle generation kinetics approach, converting target concentration into quantifiable SERS signal generation rates. This coupling of signal transduction mechanisms with chemometrics provides a novel strategy for complex matrix detection. Meanwhile, Guo *et al.*<sup>118</sup> combined BPANN with PCA-LDA, showcasing the synergistic innovation of deep learning and traditional pattern recognition methods. Nevertheless, these innovations have yet to address the fundamental challenge of establishing a universal “SERS-chemometrics” collaborative theoretical framework, rather than case-specific optimization for single targets. Future efforts should focus on the model transferability across different substances and matrices, as well as the lightweight design of algorithms for real-time detection scenarios.

### SERS-based colorimetry

Colorimetry, as a classical analytical technique, is based on the core mechanism of optical signal changes induced by specific interactions between target analytes and chromogenic reagents, typically manifested as observable changes in solution color or absorbance. Its principles can be divided into two categories: one is based on chemical reactions generating colored products (*e.g.*, metal ions forming characteristic absorption peaks through complexation with organic ligands), and the other



Fig. 9 (A) A rapid and sensitive SERS method for detecting Pb<sup>2+</sup> in food established by aptamer regulated gold nanoparticle reduction.<sup>122</sup> (B) Schematic description of deltamethrin residue detection in wheat by Ag@ZnO NF-based surface-enhanced Raman spectroscopy coupled with chemometric models.<sup>123</sup> (C) Schematic illustration of the preparation of Au nanostars and the sample detection process.<sup>124</sup> (D) Flowchart of the main data processing procedures for predicting zearalenone in maize by Raman spectroscopy.<sup>125</sup>

relies on the LSPR effect of nanomaterials. The latter is particularly important, as the LSPR wavelength of gold/silver nanoparticles undergoes significant shifts due to changes in particle size, morphology, or aggregation state, and this color change can be quantitatively correlated with target concentration through visual observation or UV-vis spectroscopy. Its sensitivity depends on the surface modification strategies and aggregation kinetics of nanoparticles, but traditional colorimetry often faces insufficient sensitivity for low-concentration analytes due to limitations in optical resolution.

The integration of colorimetry with SERS enables the construction of dual-modal sensing platforms. This combination is typically realized by designing functional nanoproboscopes. When the target analyte is present, it induces nanoparticle aggregation or dispersion to generate colorimetric signals, while simultaneously triggering strong SERS effects in the “hot spots” formed by aggregation.

At present, user-friendly colorimetry is more preferred for on-site monitoring due to the fact that color change is easy to observe and capture.<sup>126,127</sup> SERS-based colorimetric technology, as a novel optical detection technique, is increasingly popular in the identification of chemical pollutants due to its advantages

such as rapidity, readable absorption spectra, low cost, and on-site testing.<sup>39,128</sup>

For example, Song *et al.*<sup>129</sup> designed Au@AgPt octahedral core-shell nanoparticles, which achieved colorimetric detection of Hg<sup>2+</sup> through the peroxidase-like activity of the Pt shell catalyzing chromogenic reactions, while utilizing the SERS activity of the Au core for ultrasensitive quantification, demonstrating the unique advantages of heterostructured nanomaterials in dual-modal sensing (Fig. 10A). Similarly, Dai *et al.*<sup>130</sup> developed MnO<sub>2</sub>@AuNPs@aptamer (Apt) probes, where aptamer-mediated bacterial capture enhanced oxidase activity to generate colorimetric signals, while nanoparticle aggregation formed SERS “hot spots” for highly specific recognition. This coupling of biological functionalization with nanozyme activity is a typical paradigm for dual-modal integration (Fig. 10B).

Wu *et al.*<sup>131</sup> innovatively integrated magnetic Fe<sub>3</sub>O<sub>4</sub>@Au nanoproboscopes into an immunochromatographic platform, utilizing magnetic enrichment to enhance target capture efficiency and triggering both colorimetric (LSPR color change) and SERS (Raman tag signal amplification) responses through the Au shell, achieving “one-step enrichment-dual-mode output” for instant detection (Fig. 11A). Zhang *et al.*,<sup>132</sup> through the synergistic effect of EXPAR nucleic acid amplification and



Fig. 10 (A) Schematic illustration of the preparation of Au@AgPt@MCH and the colorimetric/SERS sensing strategy for Hg<sup>2+</sup>.<sup>129</sup> (B) Schematic diagram of MnO<sub>2</sub>@AuNP synthesis and the mechanism of specific *S. aureus* detection.<sup>130</sup>

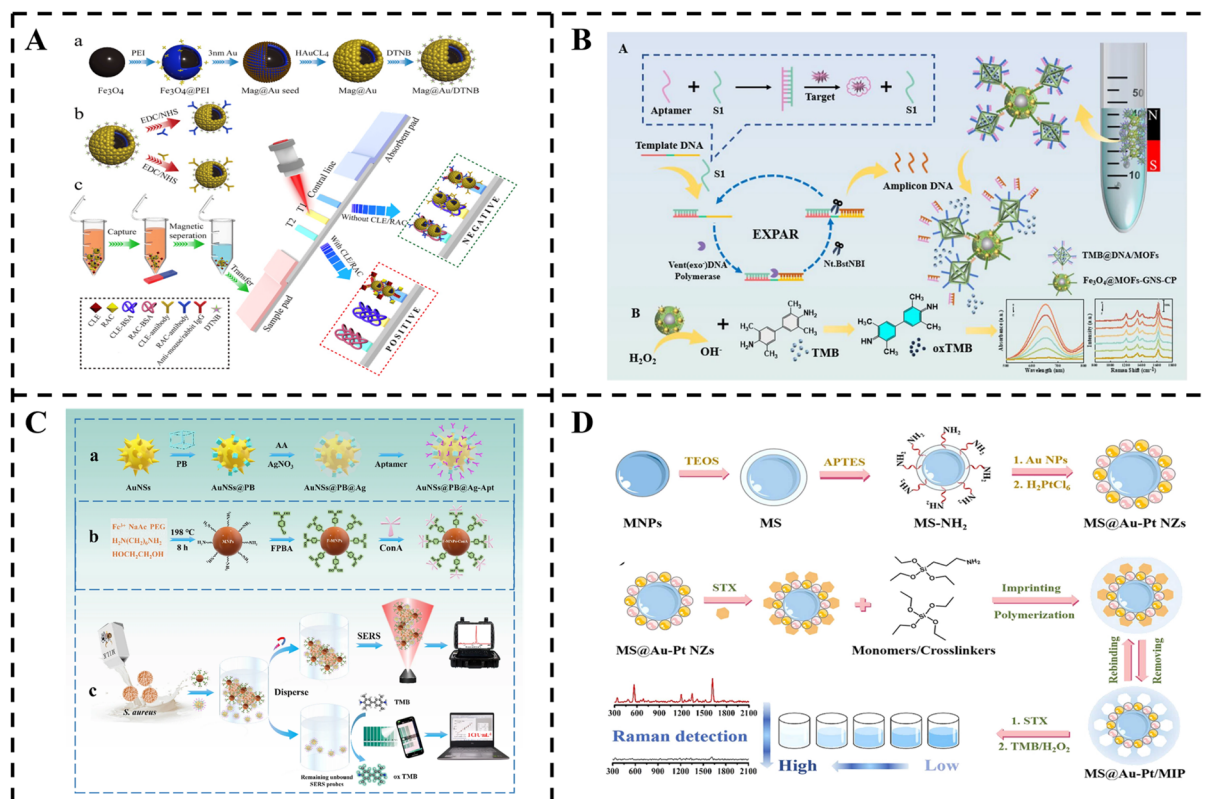


**Fig. 11** (A) Schematic of (a) the synthesis process of Mag@Au/DTNB NPs, (b) the coupling process of Mag@Au/DTNB NPs with antibodies, and (c) the detection principle based on dual-readout Mag@Au-ICA for the simultaneous detection of CLE and RAC.<sup>132</sup> (B) Principle of the dual-mode biosensor.<sup>132</sup> (C) Schematic diagram of (a) AuNSs@PB@Ag-Apt, (b) the preparation process of F-MNPs-ConA, and (c) SERS/colorimetric dual-mode intelligent biosensor for the detection of *S. aureus*.<sup>133</sup> (D) Schematic presentation of the MIDM method for the detection of STX. Preparation of magnetic nanozymes (MS@Au-Pt NZs) and MS@Au-Pt/MIP for magnetic separation and dual-mode detection of STX using the colorimetric assay and Raman method.<sup>134</sup>

bimetallic nanozymes (core-satellite structures), converted single target molecules into multiple catalytic signals, thereby constructing an ultrasensitive dual-modal sensing system with a dynamic range spanning six orders of magnitude (Fig. 11B).

In terms of probe engineering, researchers have addressed signal interference through multi-level structural optimization. Zhao *et al.*<sup>133</sup> constructed AuNSs@PB@Ag-Apt probes, embedding Prussian blue (PB) between the gold core and silver shell, leveraging PB's zero-background signal characteristics in the Raman silent region ( $2070\text{ cm}^{-1}$ ) to effectively avoid spectral overlap interference in complex matrices (Fig. 11C). Meanwhile, Wu *et al.*<sup>134</sup> designed MS@Au-Pt/MIP magnetic nanozymes, selectively capturing toxins through molecularly imprinted (MIP) cavities and synchronously regulating TMB chromogenic reactions and oxTMB Raman responses based on catalytic activity inhibition mechanisms, achieving logic detection with inversely correlated dual signals, providing a new approach for anti-interference detection (Fig. 11D).

While current SERS-colorimetric dual-modal sensing technology has achieved significant progress in signal complementarity, functional integration, and environmental adaptability, its further development still confronts critical scientific challenges. Primarily, the synergistic interaction between LSPR and EM field enhancement effects in nanoprobe

remains constrained by structural compatibility at material interfaces. Secondly, optical interference across signal channels during multi-target detection persists as an unresolved issue. Furthermore, differential attenuation phenomena of dual-modal signals under complex environmental conditions substantially compromise detection reliability. To address these challenges, future research should pursue collaborative innovation between probe design and signal interpretation.

### SERS-based fluorescence

Fluorescence analysis is based on the physical process in which molecules or nanomaterials, upon excitation by light of a specific wavelength, undergo electronic transitions from the ground state to the excited state and emit light of characteristic wavelengths upon returning to the ground state. Its mechanisms can be divided into two categories: intrinsic fluorescence (*e.g.*, spontaneous fluorescence of aromatic compounds and certain metal complexes) and extrinsic fluorescence (achieved through labeling with fluorescent dyes or quantum dots). Fluorescence intensity is positively correlated with target concentration, and the Stokes shift property effectively separates excitation and emission spectra, avoiding background interference. However, traditional fluorescence methods are susceptible to photobleaching, scattered light interference, and

limitations from autofluorescence in complex matrices, especially facing sensitivity bottlenecks in low-concentration detection. In terms of detection sensitivity, fluorescence technology itself possesses high sensitivity, capable of responding to low concentrations of analytes. Fluorescent biosensors use fluorescent substances as sensing elements. They achieve quantitative analysis of target substances *via* fluorescence intensity changes, offering advantages like simple operation, high sensitivity, speed, precision, and selectivity.<sup>135</sup>

In recent years, scholars have optimized the detection performance of traditional fluorescence methods using nanomaterials such as nano-labels. For example, Zhang *et al.*<sup>136</sup> innovatively combined microplate quantification with nitrocellulose membrane visual detection through quantum dot-labeled antibody-based dual-mode fluorescence immunoassay (FLISA), leveraging the high photostability of quantum dots to overcome the photobleaching defects of traditional organic dyes. Xue *et al.*<sup>137</sup> developed a fluorescent biosensor based on immunomagnetic nanoparticles and quantum dot probes, rapidly enriching target bacteria through high-gradient magnetic fields and significantly improving the capture efficiency of low-concentration bacteria combined with large-volume sample processing capabilities, providing a new strategy for pathogen screening in complex food matrices. Duan *et al.*<sup>138</sup> took a different approach by coupling *Salmonella typhimurium* aptamers with the  $\epsilon$  subunit of  $F_0F_1$ -ATPase, converting bacterial binding into enzyme rotational kinetic changes and achieving label-free detection through fluorescence signal attenuation induced by proton flux disturbance. This biomechanical-fluorescence signal transduction

mechanism breaks through the probe interference limitations of traditional labeling methods.

Some scholars have combined fluorescence with SERS, achieving signal complementarity and cross-validation through synergistic design of nanoprobcs. The core strategy lies in utilizing the dual functions of plasmonic nanostructures. On one hand, the LSPR effect of noble metal nanoparticles can modulate the radiative decay rate of fluorescence signals, such as achieving fluorescence enhancement (metal-enhanced fluorescence, MEF) or quenching (fluorescence resonance energy transfer, FRET) through distance regulation between the metal and fluorophores. On the other hand, "hot spots" formed by nanoparticle aggregation or surface roughening can significantly enhance the Raman signals of adsorbed molecules. Additionally, target-induced conformational changes in probes can simultaneously alter fluorescence and SERS responses. For example, aptamer-modified Ag nanoclusters exhibit fluorescence quenching due to structural rearrangement upon binding specific antibiotics, while the exposed Ag surface adsorbs Raman reporter molecules to generate specific SERS fingerprint peaks. This "one rises, the other falls" dual-signal logic relationship significantly improves detection reliability.

For instance, Rong *et al.*<sup>139</sup> coupled upconversion nanoparticles (UCNPs) with AuNPs, leveraging the anti-Stokes emission properties of UCNPs to avoid background fluorescence interference, while AuNPs served as SERS substrates to enhance Raman signals after aptamer recognition. This heterostructure design endowed the detection of phthalate esters (PAEs) with both high sensitivity and anti-matrix interference capabilities (Fig. 12A). Similarly, Gao *et al.*<sup>140</sup> constructed



Fig. 12 (A) Schematic illustration of the fluorescence and SERS bimodal nanosensor for PAEs.<sup>139</sup> (B) Schematic representation of the aptasensor based on gold nanoparticles and magnetic nanoparticles for the detection of AFB<sub>1</sub>.<sup>140</sup> (C) Analytical principle of the CdTe QD satellite FA-CdTe material for dual-mode fluorescence-SERS determination of  $UO_2^{2+}$ .<sup>141</sup> (D) Schematic illustration of the TC detection mechanism using the dual-mode nanoprobcs.<sup>142</sup>

AuNPs-MNP composite probes, where the synergistic effect of FRET and SERS effects simultaneously triggered fluorescence quenching and Raman signal enhancement upon binding of AFB<sub>1</sub> to aptamers. The inversely correlated dual signals significantly improved detection specificity (Fig. 12B).

In terms of probe engineering, researchers have achieved spatial signal separation through hierarchical structural optimization. Sun *et al.*<sup>141</sup> developed Fe<sub>3</sub>O<sub>4</sub>@SiO<sub>2</sub>@Au-CdTe core-satellite structures, utilizing the specific quenching of CdTe quantum dots' fluorescence response to uranyl ions (UO<sub>2</sub><sup>2+</sup>), while the Au shell enhanced the characteristic Raman peaks of uranyl. This "fluorescence-SERS domain-separated response" mechanism effectively avoided spectral crosstalk (Fig. 12C). Meanwhile, Qi *et al.*<sup>142</sup> designed Ag@NH<sub>2</sub>-MIL-101(Al) nanopropes, achieving fluorescence signal turn-off through the inner filter effect of metal-organic frameworks (MOFs), while  $\pi$ - $\pi$  interactions between tetracyclines (TCs) and the probes triggered SERS signal turn-on, demonstrating chemically driven dual-modal logic sensing (Fig. 12D).

From the above discussions, it is evident that these studies have made progress in signal complementarity, multifunctional probes, and anti-interference capabilities. However, the practical application of this technology still faces multiple challenges. Firstly, complex synthesis processes, such as core-shell structures, MOF encapsulation, or magnetic composite probes, limit the feasibility of mass production. Secondly, the intensity of fluorescence and SERS signals is easily affected by environmental factors (*e.g.*, pH and ionic strength), potentially causing dual-modal signal calibration deviations. Additionally, competitive adsorption of multiple components in food matrices may weaken the specificity of recognition elements on the probe surface. Future efforts should focus on standardized probe construction and deep learning-driven signal fusion algorithms to overcome current technical bottlenecks and promote the transition of this combined technology from the laboratory to on-site detection.

### SERS-based electrochemistry

EC detection is based on redox reactions initiated by target analytes on the electrode surface, achieving quantitative analysis by measuring changes in electrical signals such as current, potential, or conductivity. Its core mechanisms can be divided into two categories: direct electrochemistry (where the target itself participates in electron transfer) and indirect electrochemistry (where electron transfer is mediated by labels or nanomaterials, such as enzyme-catalyzed reactions generating electroactive substances). For example, in amperometry, the oxidation or reduction current of the target under a constant potential is linearly related to its concentration. EC impedance spectroscopy (EIS) reflects biological recognition by analyzing changes in charge transfer resistance at the electrode interface.

EC sensors are among the most used sensors, offering advantages such as high sensitivity, ease of operation, and low detection costs.<sup>143</sup> The main types include voltammetric sensors,<sup>144</sup> potentiometric sensors,<sup>145</sup> and impedance-based sensors.<sup>146</sup> To enhance the sensitivity of the electrical signal

response and reduce the detection limit, materials such as metals, multi-walled carbon nanotubes, and other inorganic materials, organic materials like MOFs,<sup>36,147</sup> and various bio-based materials are often used to modify the working electrode, meeting the needs of contaminant detection in complex food samples<sup>148,149</sup> and acquiring information on plant growth status in a timely manner.<sup>150,151</sup> In recent years, flexible substrates that are deformable and adaptable to different forms and surfaces have received increasing attention in the field of EC sensors.<sup>152,153</sup>

The core strategies for synergistic design of electrode surface functionalization and biological recognition elements can be summarized into three categories: nanomaterial engineering, biomolecular recognition, and diversification of signal amplification mechanisms.

In nanomaterial engineering, researchers optimize electrode interface performance by introducing nanostructures with high conductivity and catalytic activity. For example, Zahirifar *et al.*<sup>154</sup> used carbon nanotube-modified carbon paste electrodes to enhance the adsorption capacity of diazinon through their high specific surface area. Wang *et al.*<sup>155</sup> developed UiO-66-NH<sub>2</sub>@MWCNT composites, synergistically improving cadmium ion detection efficiency through the porous properties of MOFs and the conductivity of carbon nanotubes. Qin *et al.*<sup>156</sup> modified electrodes with Eu<sup>3+</sup>-doped Zn-MOF ultrathin nanosheets, leveraging the enrichment effect of MOFs and the fluorescence properties of rare earth ions to enhance the electron transfer efficiency of 2,6-dichloro-4-nitroaniline. Prabhu *et al.*<sup>157</sup> constructed a highly sensitive EC sensing interface for  $\alpha$ -naphthaleneacetic acid through the synergistic conductive-catalytic effects of multi-walled carbon nanotubes and Ca-ZnO composites. Meanwhile, Li *et al.*<sup>158</sup> designed a ternary nanocomposite of Au@Pt/CNHs@RGO, enhancing the oxidation response of carbendazim through the synergistic catalytic effects of noble metals and carbon-based materials. Although such nanocomposite modification strategies effectively improve sensor sensitivity, the complexity of their preparation processes and batch-to-batch material stability remain bottlenecks for practical applications (Table 4).

In the field of biomolecular recognition, researchers have significantly improved sensor selectivity by integrating specific elements such as DNAzymes, aptamers, and antibodies. Zhang *et al.*<sup>159</sup> achieved specific recognition of trace lead in leafy vegetables by combining lead ion-dependent DNAzymes with porphyrin-functionalized MOFs. Zhang *et al.*<sup>160</sup> developed an aptamer sensor based on Hg<sup>2+</sup>-induced DNA conformational changes, regulating electron transfer at the electrode interface through mercury ion-mediated DNA hairpin structural changes. Liu *et al.*<sup>161</sup> accelerated the binding kinetics of mercury ions to DNA probes through an electric field-induced pre-enrichment strategy, reducing detection time while improving sensitivity. Zhu *et al.*<sup>162</sup> constructed a label-free ratiometric EC aptamer sensor based on hybridization chain reactions, reducing matrix interference in aflatoxin B<sub>1</sub> detection through a self-calibration mechanism. The innovation in such biological recognition strategies lies in the coupling design of molecular recognition and signal transduction. For example, Huang *et al.*<sup>163</sup> combined

Table 4 Application summary of EC sensors modified with various materials for the detection of food hazards

Modified materials	Analyte	Detection matrix	Detection limit	Reference
Carbon nanotubes	Diazinon	Fruits and vegetables	$4.5 \times 10^{-10}$ mol L <sup>-1</sup>	154
UiO-66-NH <sub>2</sub> @MWCNTs	Cadmium ions	Meat	0.2 µg L <sup>-1</sup>	155
Eu <sup>3+</sup> @Zn-MOF-NS ultrathin nanosheets	2,6-Dichloro-4-nitroaniline	Vegetables	$1.7 \times 10^{-7}$ mol L <sup>-1</sup>	156
MWNTs and Ca-ZnO composite materials	$\alpha$ -Naphthylacetic acid	Fruits and vegetables	$2.5 \times 10^{-11}$ mol L <sup>-1</sup>	157
Au@Pt/CNHs@RGO	Carbendazim	Fruit and vegetable juices	$1.64 \times 10^{-9}$ mol L <sup>-1</sup>	158

DNA conformational changes with the biomimetic catalysis of PorMOF, controlling signal amplification by regulating the distance between catalytic active sites and the electrode through silver ion-induced DNA folding. However, the environmental stability of biological recognition elements and non-specific adsorption in complex food matrices still need further resolution.

The diversification of signal amplification mechanisms is another notable trend. Liu *et al.*<sup>164</sup> developed an EC-PEC dual-modal ratiometric sensor, improving the reliability of patulin detection through mutual verification of photoelectrochemical (PEC) and EC signals. Li *et al.*<sup>165</sup> combined conductive hydrogels with LSPR, enhancing the oxidation current of methylene blue through photoexcitation for ultrasensitive detection of aflatoxin B<sub>1</sub>. Murasova *et al.*<sup>166</sup> converted bacterial capture events into EC release signals of metal ions through cascade signal amplification using quantum dot-labeled antibodies and dendritic polymers. Zhu *et al.*<sup>167</sup> prepared highly specific monoclonal antibodies through cell fusion technology, constructing an EC immunosensor using a competitive immunoassay strategy, with a wide dynamic range and low detection limit suitable for precise monitoring of trace contaminants in complex food matrices. These strategies break through the dynamic range limitations of traditional EC detection through physico-chemical synergistic amplification mechanisms, but the integration of multiple components also increases the complexity of sensor design and operation.

The combination of electrochemistry with SERS offers significant advantages in the field of analytical detection. On one hand, it enhances detection sensitivity: SERS can greatly amplify Raman signals, and the EC process can modulate the surface properties of the substrate by altering the electrode potential, synergistically further amplifying the signal with SERS. Additionally, controlling the potential can enrich target analytes on the electrode surface, thereby increasing the intensity of the SERS signal. On the other hand, it improves detection selectivity: EC-induced specific reactions screen for the target substances, and potential control can modulate the adsorption of different substances. Moreover, it enables *in situ* and real-time monitoring, dynamically tracking the EC reaction for dynamic analysis. This combined technology also expands the detection range, activating inherently difficult-to-detect inert molecules, and adapts to various special systems. It also simplifies the detection process, eliminating the need for complex pretreatment of some samples.

For example, Han *et al.*<sup>168</sup> combined EC self-assembly with diazo reactions, optimizing the distribution density of AuNPs

on the electrode surface to simultaneously enhance the SERS signal and EC response of nitrite, constructing an integrated sensing interface for “*in situ* reaction-dual-mode detection” (Fig. 13A). Tang *et al.*<sup>169</sup> enhanced the van der Waals forces between acetamiprid (AAP) and AgNPs by applying a potential of  $-0.7$  V, increasing the SERS signal by 5-fold, and revealed the regulatory mechanism of the electric field on molecular adsorption behavior using density functional theory (DFT) (Fig. 13B). Similarly, Wu *et al.*<sup>170</sup> utilized electrodeposition to grow AuNPs *in situ* on indium tin oxide (ITO) electrodes, applying a potential of  $+0.3$  V to increase the SERS intensity of AAP by 4-fold, while verifying the influence of molecular adsorption orientation on Raman signals under an electric field through DFT simulations (Fig. 13C). Tang *et al.*<sup>171</sup> further designed Ag@SiO<sub>2</sub> core-shell nanospheres as SERS substrates, enhancing the characteristic peak intensity by 4.3-fold through strengthened intermolecular forces at a potential of  $-0.5$  V, while improving substrate stability by protecting the nano-structured silver with a SiO<sub>2</sub> dielectric layer (Fig. 13D).

These studies break through the sensitivity limitations of traditional SERS detection by precisely controlling electrode potential to enhance target adsorption or alter molecule-substrate interactions. Integrating the EC cell with Raman detection enables real-time monitoring of signal evolution under potential regulation, simplifying the operational process. Simultaneously, DFT calculations provide theoretical support for the signal enhancement mechanism by analyzing the influence of the electric field on molecular adsorption configurations. Additionally, the reliability of detection is validated through HPLC-MS comparisons. However, these strategies may face new challenges: potential application may cause structural reconstruction of nano-substrates (*e.g.*, oxidation of AgNPs), leading to decreased SERS signal stability.

### SERS-based molecularly imprinted polymers

Molecular imprinting technology (MIT) is a chemical synthesis method based on the principle of biomimetic recognition, with its core being the synthesis of polymer materials (MIPs) with specific recognition sites under the guidance of template molecules. Its principle is like the “lock and key” specific recognition mechanism between enzymes and substrates or antibodies and antigens in nature. Initially, template molecules form complexes with functional monomers through non-covalent or covalent interactions. Subsequently, polymerization occurs in the presence of cross-linkers and initiators, forming a highly cross-linked polymer network.<sup>172</sup> The template molecules are then eluted from the polymer, leaving cavities



Fig. 13 (A) Schematic representation of the developed SERS sensing strategy for nitrite detection.<sup>168</sup> (B) The schematic presentation of the strategy for EC-SERS detection of AAP using SPE modified with AgNPs (SERS enhancement at  $-0.7$  V and DFT model).<sup>169</sup> (C) Schematic presentation of the preparation of the AuNPs/ITO SERS substrate and EC-SERS detection of AAP with an applied potential at  $+0.3$  V.<sup>170</sup> (D) Schematic presentation of EC-SERS involved in the preparation of Ag@SiO<sub>2</sub>NPs, the incubation of AAP with the substrate and the enhanced detection of AAP at  $-0.5$  V.<sup>171</sup>

complementary to the template molecules in shape, size, and chemical groups. These cavities selectively recognize template molecules and their analogs, enabling specific binding with target molecules.<sup>173,174</sup> The performance of MIPs is synergistically regulated by the structure of the template molecule, the ratio of functional monomers, the type of cross-linker, and the solvent environment. Their selectivity and binding capacity essentially stem from the stereo-complementarity of molecular recognition cavities and the specific interactions between functional groups and target molecules. Due to its high selectivity, stability, and reproducibility, molecular imprinting technology has been widely applied in various fields such as food detection, drug analysis, environmental monitoring, and biomedicine.<sup>172,175</sup>

Research on the application of molecular imprinting technology in food detection has demonstrated its potential to address the detection of target analytes in complex matrices through multidimensional innovations. For example, the virtual template strategy proposed by Zhang *et al.*<sup>176</sup> effectively avoids interference from template molecule residues, but the universality of its conformational simulation of template molecules and its selectivity in more complex food systems still require further validation (Fig. 14A). The imprinted membrane constructed by Dong *et al.*<sup>177</sup> through synergistic modification of functional materials and click chemistry achieves high adsorption capacity while improving anti-fouling properties, but the long-term stability of the membrane material and the feasibility of large-scale preparation have not been

systematically studied, potentially limiting its practical industrial application (Fig. 14B). Su *et al.*<sup>178</sup> and Yang *et al.*<sup>179</sup> significantly improved detection sensitivity using radiometric sensing (Fig. 14C) and nanocomposite probe strategies (Fig. 14D), respectively. However, the former relies on an indirect detection mechanism based on metal ion redox reactions, which may be interfered with by coexisting oxidizing substances, while the latter's sensor preparation process based on the sol-gel method is relatively complex, both posing challenges to method standardization.

Some scholars have attempted to integrate MIT with EC and fluorescence techniques. For example, when MIT is combined with electrochemistry (*e.g.*, GO/AgNPs-MIPs by Qin *et al.*<sup>180</sup> and Au@MIP membranes by Han *et al.*<sup>181</sup>), sensing interfaces are constructed using nanocomposite materials, significantly enhancing detection sensitivity through EC signal amplification while leveraging the selective enrichment of MIT to reduce non-specific adsorption in electrochemistry. However, insufficient research on the stability and long-term reusability of the imprinted layer on the electrode surface may affect persistent detection performance in practical scenarios.<sup>180,181</sup> In fluorescence-MIT integration direction (*e.g.*, carbon dot-MIP composite probes by Liu *et al.*<sup>182</sup> and ratiometric fluorescence sensors by Li *et al.*<sup>183</sup>), “switch-type” signal responses or dual-channel self-calibration strategies retain the high selectivity of MIT while avoiding background interference in fluorescence detection, even enabling rapid visual screening.<sup>182–187</sup> (Fig. 15A–F). However, the long-term effects of the photostability of



Fig. 14 (A) Schematic illustration of the process for preparation of dex-MMIPs.<sup>176</sup> (B) Schematic illustration of constructing LINMIMs for selective recognition and separation of lincomycin.<sup>177</sup> (C) Schematic diagram of MIP/MWCNTs-Au/GCE for GLY indirect determination, in which the Cu(II)-GLY complex is well formed.<sup>178</sup> (D) Schematic diagram of the MIP preparation process.<sup>179</sup>

fluorescent probes and endogenous fluorescence interference in complex matrices have not been systematically validated.

Compared to electrochemistry and fluorescence, the integration of MIT with SERS provides a new approach for the

precise detection of target analytes in complex matrices through the synergistic effects of selective enrichment and signal amplification. The high sensitivity and fingerprint recognition characteristics of SERS effectively compensate for the



Fig. 15 (A) Illustration of the preparation of MIP-coated CDs.<sup>182</sup> (B) Schematic illustration for the preparation of SiO<sub>2</sub>-MPTMS@FMIPs.<sup>184</sup> (C) Schematic procedure for the preparation of SiO<sub>2</sub>@QDs@MIPs.<sup>185</sup> (D) Flow chart of the preparation of N-CDs@MIPs.<sup>186</sup> (E) Schematic illustration of the preparation of turn-on MIFS and detection of HRP based on boronate affinity sandwich assay and nanoparticle signal amplification.<sup>187</sup> (F) Schematic illustration for the one-pot preparation process of a nanoscale core-shell structured FA imprinted ratiometric fluorescence sensor (namely FL-MIPs) and possible detection principle.<sup>183</sup>

limitations of MIT in trace detection, while the selective enrichment of MIT can suppress non-specific adsorption interference in SERS. For example, when SERS-active substrates are integrated with MIT layers, MIT can directionally capture target molecules and enrich them in SERS “hot spots,” achieving ultrasensitive detection through Raman signal amplification (e.g., Li *et al.*<sup>188</sup> rapidly detected pesticide residues in apples using magnetic MMIP-SERS) (Fig. 16A). Ju *et al.*<sup>189</sup> prepared imprinted polymers using precipitation polymerization (Fig. 16B), Guo *et al.*<sup>190</sup> designed flexible Au@AgNCs/PDMS-MIP arrays (Fig. 16C), and Hui *et al.*<sup>191</sup> proposed a magnetic solid-phase extraction-SERS integration strategy, further expanding the application potential of this technology in on-site food screening (Fig. 16D).

The core of such integrated technologies lies in the integration strategies of MIT and SERS substrates, mainly including surface modification, *in situ* synthesis, template methods, magnetic nanoparticle methods, and flexible substrate methods. For example, Kim *et al.*<sup>192</sup> synthesized MIT-SERS composite substrates *in situ* on flexible cellulose nanofibers using polymer micelle EC deposition, while Xie *et al.*<sup>193</sup> constructed 3D Au@PDMS substrates through self-assembly and modified them with MIT layers. These methods balance selectivity and signal intensity by optimizing interface structures (e.g., controlling MIT layer thickness and SERS-active site distribution), significantly improving detection sensitivity and anti-interference capabilities.

Nevertheless, the integration of MIT-SERS still faces challenges. Firstly, MIT layers may obscure SERS-active sites,

requiring precise control of material micro-nano structures. Secondly, most current studies focus on single targets, lacking validation for simultaneous detection of multiple contaminants. Finally, the batch stability of substrates, suppression of complex matrix interference, and cost control in practical applications still require systematic optimization. Future research should focus on precise control of material micro-nano structures, multi-template imprinting strategies, and standardized signal calibration methods to promote the substantial transition of MIT-SERS from laboratory innovation to industrial applications.

Notably, MIP-based SERS sensors not only excel in food detection but also provide potential solutions for biomedical applications due to their high sensitivity and anti-interference properties. Arabi *et al.*<sup>173</sup> achieved absolute recognition of chiral molecules using an “inspector” recognition mechanism (IRM) based on the permeability changes of polydopamine (PDA) imprinted layers, eliminating the reliance on molecular structures in traditional methods. Chen *et al.*<sup>194</sup> focused on large-size protein detection, achieving precise quantification by dynamically monitoring the state of imprinted cavities to suppress non-specific adsorption. Arabi *et al.*<sup>195</sup> developed a label-free universal sensor, where target proteins block signal pathways, resulting in a negative correlation between SERS signals and concentration, achieving ultrasensitive detection in complex biological samples. These strategies, through dynamic signal regulation and multi-level structural innovation, provide highly sensitive and specific detection platforms for disease marker analysis and drug chiral recognition.



Fig. 16 (A) Analysis of myclobutanil and tebuconazole in apple by a novel SERS method based on MMIP-SERS.<sup>188</sup> (B) Schematic of the preparation process of imprinted polymers and MIPs-SERS for extracting and detecting nitenpyram.<sup>189</sup> (C) The synthesis and SERS detection process of AAP-MIMs.<sup>190</sup> (D) Schematic illustration for the preparation process of MGO@MIP particles and their application in ofloxacin detection using SERS signals.<sup>191</sup>

### SERS-based microfluidic chip

Microfluidic technology is based on the precise manipulation of fluids within micro-scale channels, with its core principles involving laminar flow effects, capillary actions dominated by surface tension, and enhanced diffusive mass transfer. At the microscale, the Reynolds number of fluids is extremely low (typically  $Re < 1$ ), where viscous forces dominate inertial forces, resulting in stable laminar flow. This ensures that the mixing of samples and reagents primarily relies on diffusion rather than turbulence, enabling controlled mass transfer processes. Microfluidic chips are fabricated using techniques such as photolithography, soft lithography, or 3D printing, integrating microvalves, micropumps, and detection units to achieve automated sample injections, separation, reaction, and detection. Its mechanism can be summarized as “miniaturization, integration, and automation.” The advantages of this technology include high-throughput analysis, low reagent consumption (nanoliter to microliter scale), and rapid reaction kinetics, but it faces challenges such as channel clogging, surface contamination, and complex manufacturing processes.<sup>196</sup>

Compared to label-free SERS detection, label-dependent SERS biosensors can offer a very low LOD, but they still require relatively complex operational procedures at the expense of smaller equipment, which has been gradually improved by microfluidic chips.<sup>94</sup> The combination of SERS and microfluidic technology can address multiple issues. First, in terms of sample handling and analysis efficiency, microfluidic technology can precisely manipulate microsamples, combined

with the high sensitivity of SERS, improving sample utilization and accelerating the mixing reaction of samples and reagents in microchannels for rapid analysis. Second, in terms of detection sensitivity and stability, microfluidic systems can precisely control environmental conditions, enhancing the stability and repeatability of SERS signals, and can precisely mix nano-materials with samples to optimize “hot spot” formation, thereby improving detection sensitivity. Third, for multiplex detection and high-throughput analysis, the multi-channel structure of microfluidic chips can perform SERS detection on different target substances simultaneously, combined with automated operations and the rapid detection capability of SERS, to achieve high-throughput analysis. Finally, in terms of portability and on-site detection capability, microfluidic technology contributes to the miniaturization of equipment and can be combined with SERS to develop portable devices, meeting the needs for rapid and real-time on-site detection and saving time costs.

The core mechanism of integrating SERS with microfluidic technology lies in the *in situ* construction of SERS-active substrates and the enhancement of dynamic regulation capabilities for target analytes by microfluidics. For example, Yan *et al.*<sup>197</sup> generated silver nanostructures *in situ* through a one-step replacement reaction within microfluidic channels, utilizing the reaction time gradient controlled by laminar flow to regulate the size distribution of nanoparticles. This resulted in the formation of optimal SERS hotspots 2 mm from the channel inlet, enabling rapid and highly sensitive detection of mercury ions. This strategy significantly simplifies the preparation process of traditional SERS substrates (Fig. 17A).



Fig. 17 (A) A schematic of a microfluidics-assisted SERS sensor.<sup>197</sup> (B) Schematic diagram of a microfluidic system combining SERS with a microfluidic system for the determination of glyphosate in tap water.<sup>199</sup> (C) Diagram of the SERS nanosensor integrated with a microfluidic chip based on Au@Ag HNSs for GSM detection.<sup>198</sup> (D) The preparation of gold nanostar@4-mercaptopbenzoic acid@goldnanoshell structures (AuNSs@4-MBA@Au) and their utility in combination with CRISPR/Cas12a for SERS-based bacterial detection for both in-tube and  $\mu$ PAD detection. DNA1 and DNA2 were colored in blue and red, respectively, and linker ssDNA in green.<sup>201</sup>

Similarly, Gong *et al.*<sup>198</sup> designed a herringbone-shaped microfluidic channel to optimize the contact efficiency between Au@Ag hollow nanoshells (Au@Ag HNSs) and geosmin (GSM) by adjusting the flow rate and channel length. The high surface charge density and cavity structure synergistically enhanced the Raman signal. Meanwhile, the fluid shear force in microfluidics prevented nanoparticle aggregation, ensuring detection reproducibility (Fig. 17B).

In terms of complex sample processing, Emonds-Alt *et al.*<sup>199</sup> integrated the synthesis of SERS substrates for glyphosate detection and the detection process into a single microfluidic system. By optimizing reaction parameters (*e.g.*, mixing time and pH) using experimental design methods, the diffusion-dominated mass transfer characteristics of microchannels enhanced the binding efficiency between target analytes and substrates (Fig. 17C).

The rapidly evolving clustered regularly interspaced short palindromic repeat (CRISPR)-associated (CRISPR/Cas) system has become an efficient toolbox to address the need for on-site and time-effective detection.<sup>200</sup> Zhuang *et al.*<sup>201</sup> developed an RPA-Cas12a- $\mu$ PAD paper-based microfluidic chip, converting nucleic acid signals of Salmonella into detectable SERS signals through RPA isothermal amplification and the specific cleavage activity of CRISPR/Cas12a (Fig. 17D). The porous cellulose fibers not only served as fluid-driven carriers but also enriched CRISPR-activated Raman reporter molecules through capillary action, achieving ultrasensitive detection within 45 minutes.

These studies regulate the morphology and distribution of nanostructures through channel geometry design and fluid parameter control. Additionally, they leverage microscale effects (*e.g.* enhanced diffusion and shear force-induced orientation) to improve the interaction efficiency between target analytes and hotspots. Efforts are also made to integrate nucleic acid amplification, chemical reactions, and optical detection into a single chip, reducing external operational interference. However, the mechanical strength and long-term storage stability of paper-based microfluidics are insufficient, potentially affecting SERS signal consistency. The *in situ* synthesis of metal nanostructures is susceptible to fluctuations in ionic strength within the fluid, leading to uneven hotspot distribution. Furthermore, most studies are still limited to single-target detection, lacking the capability for multi-component parallel analysis. Future work should focus on developing programmable microfluidic-SERS platforms, combining deep learning algorithms for multi-channel signal analysis to expand their applicability in complex food matrices.

## Others

Current technological innovations in the field of food safety detection exhibit a significant trend toward multi-modal sensing integration and functional material-driven approaches, with commonalities reflected in the synergistic design of nanomaterial engineering, biological recognition elements, and intelligent response mechanisms to overcome the limitations of traditional detection methods.<sup>202</sup> For example, EIS technology enhances detection accuracy through

characteristic frequency screening and data fusion: Li *et al.*<sup>203</sup> established a predictive model based on the strong correlation between plant impedance spectral characteristic frequencies and phosphorus content, while Sun *et al.*<sup>204</sup> proposed a fish freshness grading method based on the fusion of EIS parameters and physicochemical indicators. Their multi-dimensional data fusion strategy improved classification accuracy by 9.2–15%.

Such studies highlight the potential of EIS in non-destructive evaluation of food quality, but its practical application is still limited by the universality of complex electrical models and the influence of environmental temperature and humidity fluctuations.

In the field of intelligent packaging, researchers have achieved visual monitoring of food spoilage through the combination of edible functional films and EC writing technology. Zhai *et al.*<sup>205</sup> developed a gelatin-gellan gum-RRA composite film that indicates spoilage in milk and fish through pH-responsive color changes, with EC writing functionality enabling patterned information encoding on the packaging. Yang *et al.*<sup>206,207</sup> integrated ammonia sensing, photostability, and antibacterial functions through the synergistic design of GN-ZnO nanoparticles and agar bilayer films, while enhancing barrier properties using TiO<sub>2</sub>. These studies embody the integrated design concept of “sensing-preservation-information interaction,” but the mechanical strength and long-term stability of edible films still require optimization, especially as they are prone to material degradation under high temperature and humidity conditions.

PEC sensors achieve ultrasensitive detection through photogenerated carrier regulation and signal amplification strategies.<sup>208,209</sup> Luo *et al.*<sup>210</sup> constructed a ZnO-NGQD composite material that enhanced PEC signals by 8.8 times for the trace detection of ZEN. Du *et al.*<sup>211</sup> developed an AgBr/Ti<sub>3</sub>C<sub>2</sub> Schottky interface sensor that achieved picogram-level detection of chlorpyrifos (0.33 pg L<sup>-1</sup>) by improving light absorption and charge separation efficiency. The ratiometric PEC immunosensor of Meng *et al.*<sup>212</sup> and the photothermal-EC dual-modal chip of Wang *et al.*<sup>213</sup> further improved reliability through signal self-calibration and multi-physical field responses. However, PEC technology generally faces challenges such as poor stability of photoelectrode materials (*e.g.*, ZnO photocorrosion) and background interference in complex food matrices. Lai *et al.*<sup>214</sup> pioneered a zero-gate-voltage organic PEC transistor aptasensor utilizing ZnO nanorod arrays, where nanostructured interface engineering coupled with transistor signal amplification enabled ultrasensitive detection of T-2 toxin. This approach demonstrated superior performance to conventional PEC methods, validated by high recovery rates and stability in complex milk matrices, offering a new bias-free sensing platform for food safety monitoring.

In terms of innovative technological exploration, Zhang *et al.*<sup>215</sup> developed a MOF-loaded antibacterial vanillin formulation that achieves controlled release of phytochemicals through humidity-triggered hydrogen bond breaking. Its molecular implantation mechanism precisely disrupts bacterial membrane structures and virulent gene transcription,

providing a new approach for active packaging. The TiO<sub>2</sub> nanopore membrane sensor of Huang *et al.*<sup>216</sup>, combined with PCA and PLS models, achieved visual quantification of trimethylamine (TMA) in lamb, offering a non-invasive solution for gas detection through a multi-color response strategy. Park *et al.*<sup>217</sup> innovatively integrated acoustofluidics with SERS, using acoustic radiation forces to directly enrich and arrange bacteria in microchannels. By specifically labeling bacterial surface biomarkers with antibody-conjugated SERS nanotags and measuring population-averaged Raman signals under flow conditions, they achieved rapid and highly reproducible quantitative detection of sepsis pathogens without the need for lysis or culture, addressing the signal fluctuations caused by laser focus volume limitations in traditional SERS detection.

## Challenges and prospects

Based on the principles introduced and case analyses above, it is necessary to combine SERS with fluorescence, colorimetry, electrochemistry, microfluidics, MIPS, and other technologies. This integration can enhance detection performance by increasing sensitivity through different principles, accurately detecting trace substances through complementary signal enhancement mechanisms, and improving specificity by leveraging the unique recognition advantages of each technology.

Despite the significant potential of SERS-integrated technologies in food safety detection, their practical application still faces multiple challenges. Firstly, non-specific adsorption in complex food matrices limits selectivity. For example, in colorimetric-SERS dual-modal detection, surface modifications of nanoprobe are easily interfered with by lipids or proteins, leading to false-positive signals. Secondly, batch variability in SERS substrates and the complexity of microfluidic chip manufacturing processes make it difficult to standardize detection results. Additionally, most existing technologies rely on laboratory equipment, making it challenging to meet the portability requirements for on-site rapid testing. To address these bottlenecks, the emergence of many new technologies offers potential breakthroughs.

For instance, using the recently developed CRISPR-Cas-based nucleic acid detection system is a promising method. In cancer diagnostics, CRISPR-Cas shows potential for highly sensitive tumor marker detection, enabling early screening to enhance cure rates and patient survival. CRISPR is a prokaryotic immune system that provides adaptive immunity against foreign nucleic acids, including phages and plasmids.<sup>218</sup> It is a complex system involving multiple genes, including Cas genes and CRISPR arrays, which consist of repeats separated by unique sequences called spacers. These spacers are derived from viral or plasmid DNA encountered by bacteria and are integrated into their genomes as a defense mechanism against future invasions.<sup>219</sup> Studies have shown that the combination of CRISPR-Cas systems with SERS can significantly enhance detection performance. For example, Kim *et al.*<sup>220</sup> achieved simultaneous detection of multidrug-resistant bacteria (*e.g.*, *Staphylococcus aureus* and *Acinetobacter baumannii*) without

nucleic acid purification or amplification steps by integrating the gene-specific recognition capability of CRISPR-Cas systems with magnetic nanoparticle-targeted enrichment and SERS signal amplification. They also utilized a three-dimensional nanopillar array swab for on-site rapid capture and diagnosis.

The integration of microfluidic technology further promotes detection automation. For instance, Xiong *et al.*<sup>221</sup> integrated bio-conjugated magnetic nanochains with dual functions of active mixing and target capture into a planar microfluidic chip. By using magnetic fields to drive the nanochains, they achieved rapid liquid-phase mixing and specific biological separation simultaneously, breaking through the limitations of traditional solid-liquid interface diffusion and significantly enhancing detection specificity.

The introduction of artificial intelligence technology further optimizes data analysis. For example, Kim *et al.*<sup>222</sup> designed specifically functionalized SERS substrates (antibody-targeted capture of amyloid- $\beta$  and dipole interaction separation of metabolites) to capture different biomarkers directionally. They utilized deep learning to automatically extract key features from complex spectra to eliminate biological fluid interference, significantly improving detection specificity through feature generalization and interpretability verification. In clinical medicine, this contributes to enhanced diagnostic accuracy and efficiency while reducing human errors. Furthermore, by analyzing large-scale patient data, AI-assisted SERS detection can identify novel biomarkers and disease association patterns, offering insights into disease pathogenesis and informing the development of innovative treatment strategies.

The development of flexible substrates is crucial for advancing materials and biosensing fields. For instance, graphene coated with nanoparticles has been used to fabricate wearable optical sensors that measure human pulse and blood oxygen levels through ambient light penetrating tissues, providing a potential platform for healthcare monitoring.<sup>223</sup> Microneedle (MN) patches, composed of needle-like structures and substrates, can penetrate the stratum corneum of plants<sup>224</sup> or humans<sup>225</sup> in a minimally invasive manner. This technology has been integrated with various detection methods such as surface-enhanced Raman spectroscopy, EC sensing, and colorimetric analysis to achieve *in situ* capture and precise analysis of biochemical signals in complex environments.<sup>226</sup> Yi *et al.*<sup>227</sup> designed a stepped microneedle patch that integrates needle tips penetrating the stratum corneum to detect internal pesticide residues in agricultural products and a substrate contacting the surface to capture external residues. Combined with the rapid adsorption and SERS signal enhancement properties of silver nanoparticles/hydrogels, they achieved simultaneous minimally invasive detection of surface and internal pesticide residues in agricultural products using a single device, overcoming the limitations of traditional methods such as complex operations and contamination risks during separate detection. If microneedle structures can be directly formed on flexible substrates, the difficulties of transferring microneedle structures to flexible substrates in traditional 3D printing can be reduced, making the microneedle structures more integrated and improving the stability and reliability of the process.

In terms of performance enhancement, the development of new SERS substrate materials, optimization of nanostructures, combination with advanced molecular recognition technologies such as aptamers and molecular imprinting, and the development of effective signal amplification strategies are necessary to achieve higher sensitivity and specificity for the precise detection of trace targets. In data analysis, the introduction of artificial intelligence algorithms and machine learning<sup>228</sup> is essential for real-time data analysis and interpretation and for constructing automated detection processes, reducing human operational errors and enabling on-site rapid detection. In the future, breakthroughs in SERS-integrated technologies will rely on ternary synergistic innovation involving nanotechnology, biotechnology, and information technology. For example, MOF materials loaded with CRISPR-Cas systems as “smart probes” can simultaneously achieve target recognition and signal amplification, while quantum computing-assisted spectral analysis algorithms are expected to enhance detection throughput. The integration of these technologies will not only reshape food safety monitoring systems but also generate profound social value in fields such as environmental governance and precision medicine.

## Data availability

No primary research results, software or code have been included and no new data were generated or analysed as part of this review.

## Author contributions

Jiaqian Liu, Xiaowei Huang: writing – original draft, writing – review & editing, and visualization. Yuerong Feng, Zhecong Yuan and Shujie Gao: writing – review & editing. Xinai Zhang, Jiyong Shi, and Xiaobo Zou: writing – review & editing and supervision. All authors have read and agreed to the published version of the manuscript.

## Conflicts of interest

There are no conflicts to declare.

## Acknowledgements

We deeply appreciate the valuable guidance and unwavering support provided by our teachers and classmates.

## Notes and references

- 1 T. Yu, Z. Suo, J. Zhu, Y. Xu, W. Ren, Y. Liu, H. Wang, M. Wei, B. He and R. Zhao, *Anal. Chim. Acta*, 2025, **1338**, 343609.
- 2 F. Chamorro, M. Carpena, M. Fraga-Corral, J. Echave, M. S. Riaz Rajoka, F. J. Barba, H. Cao, J. Xiao, M. A. Prieto and J. Simal-Gandara, *Food Chem.*, 2022, **370**, 131315.
- 3 S. A. M. Khalifa, M. Elashal, M. Kieliszek, N. E. Ghazala, M. A. Farag, A. Saeed, J. Xiao, X. Zou, A. Khatib, U. Göransson and H. R. El-Seedi, *Trends Food Sci. Technol.*, 2020, **97**, 300–316.
- 4 Y. W. Rong, M. M. Hassan, Q. Ouyang and Q. S. Chen, *Compr. Rev. Food Sci. Food Saf.*, 2021, **20**, 3531–3578.
- 5 F. Han, X. Huang and G. K. Mahunu, *Trends Food Sci. Technol.*, 2017, **59**, 37–48.
- 6 H. Jiang, R. Tan, M. Jin, J. Yin, Z. Gao, H. Li, D. Shi, S. Zhou, T. Chen, D. Yang and J. W. Li, *Biomed. Environ. Sci.*, 2022, **35**, 518–527.
- 7 N. F. D. Silva, M. M. P. S. Neves, J. M. C. S. Magalhães, C. Freire and C. Delerue-Matos, *Trends Food Sci. Technol.*, 2020, **99**, 621–633.
- 8 S. Zhang, Y. Huang, M. Chen, G. Yang, J. Zhang, Q. Wu, J. Wang, Y. Ding, Q. Ye, T. Lei, Y. Su, R. Pang, R. Yang and Y. Zhang, *Int. J. Food Microbiol.*, 2022, **378**, 109805.
- 9 J. Beyuo, L. N. A. Sackey, C. Yeboah, P. Y. Kayoung and D. Koudadje, *Discover Agriculture*, 2024, **2**, 123.
- 10 X. Zhang, X. Huang, Z. Wang, Y. Zhang, X. Huang, Z. Li, M. Daglia, J. Xiao, J. Shi and X. Zou, *Chem. Eng. J.*, 2022, **429**, 132243.
- 11 E. C. Scutarasu and L. C. Trinca, *Foods*, 2023, **12**, 3340.
- 12 P. Verzelloni, T. Urbano, L. A. Wise, M. Vinceti and T. Filippini, *Environ. Pollut.*, 2024, **345**, 123462.
- 13 R. M. Speer, X. Zhou, L. B. Volk, K. J. Liu and L. G. Hudson, in *Advances in Pharmacology*, ed. M. Costa, Academic Press, 2023, vol. 96, pp. 151–202.
- 14 O. E. Eteng, C. A. Moses, E. I. Ugwor, J. E. Enobong, A. J. Akamo, Y. Adebekun, A. Iwara and E. Ubana, *Egypt. J. Basic Appl. Sci.*, 2021, **9**, 11–22.
- 15 Y. Zhao, X. Jing, F. Zheng, Y. Liu and Y. Fan, *Anal. Chem.*, 2021, **93**, 8945–8953.
- 16 M. F. Ahmad, F. A. Ahmad, A. A. Alsayegh, M. Zeyauallah, A. M. Alshahrani, K. Muzammil, A. A. Saati, S. Wahab, E. Y. Elbendary, N. Kambal, M. H. Abdelrahman and S. Hussain, *Heliyon*, 2024, **10**, e29128.
- 17 K. Jomova, S. Y. Alomar, E. Nepovimova, K. Kuca and M. Valko, *Arch. Toxicol.*, 2024, 1–57.
- 18 N. Taprab and Y. Sameenoi, *Anal. Chim. Acta*, 2019, **1069**, 66–72.
- 19 M. Sepahvand, F. Ghasemi and H. M. Seyed Hosseini, *Food Chem. Toxicol.*, 2021, **149**, 112025.
- 20 D. Tibebe, M. Hussien, M. Mulugeta, D. yenealem, Z. Moges, M. Gedefaw and Y. Kassa, *BMC Chem.*, 2022, **16**, 87.
- 21 Z. Alinezhad, M. Hashemi and S. B. Tavakoly Sany, *PLoS One*, 2024, **19**, e0296649.
- 22 H. Lu, G. Huang, D. Wang, Q. Ma, Y. Zhang, M. Jin and L. Shui, *Chem. Commun.*, 2024, **61**, 1657–1660.
- 23 B. Zhang, W. T. Liu, Z. J. Liu, X. L. Fu and D. L. Du, *Eur. Food Res. Technol.*, 2022, **248**, 109–117.
- 24 H. Dong, Y. Xu, H. Ye, M. Huang, J. Hu, Y. Xian, X. Zeng, W. Bai and D. Luo, *Food Anal. Methods*, 2021, **15**, 17.
- 25 R. Deng, J. Bai, H. Yang, Y. Ren, Q. He and Y. Lu, *Coord. Chem. Rev.*, 2024, **506**, 215745.
- 26 K. Zeng, B. Chen, Y. X. Li, H. Meng, Q. Y. Wu, J. Yang and H. F. Liang, *Int. J. Food Sci. Technol.*, 2022, **57**, 6028–6037.
- 27 M. M. Yin, W. J. Wang, J. Wei, X. M. Chen, Q. S. Chen, X. Chen and M. Oyama, *Food Chem.*, 2022, 368.

- 28 Z. J. Liu, X. Y. Wang, X. X. Ren, W. B. Li, J. F. Sun, X. W. Wang, Y. Q. Huang, Y. G. Guo and H. W. Zeng, *Food Chem.*, 2021, **355**, 129633.
- 29 W. W. Wu, W. Ahmad, M. M. Hassan, J. Z. Wu, Q. Ouyang and Q. S. Chen, *Food Chem.*, 2024, 437.
- 30 W. R. Zhu, L. B. Li, Z. Zhou, X. D. Yang, N. Hao, Y. S. Guo and K. Wang, *Food Chem.*, 2020, **319**, 126544.
- 31 Z. Y. Gan, W. Zhang, M. Arslan, X. T. Hu, X. A. Zhang, Z. H. Li, J. Y. Shi and X. B. Zou, *J. Agric. Food Chem.*, 2022, **70**, 10065–10074.
- 32 Y. Cheng, M. Qin, P. Li and L. Yang, *RSC Adv.*, 2023, **13**, 4584–4589.
- 33 Q. Wei, Q. Dong and H. Pu, *Biosensors*, 2023, **13**(2), 296.
- 34 M. M. Hassan, W. Ahmad, M. Zareef, Y. Rong, Y. Xu, T. Jiao, P. He, H. Li and Q. Chen, *Food Chem.*, 2021, **358**, 129844.
- 35 W. L. Zhai, T. Y. You, X. H. Ouyang and M. Wang, *Compr. Rev. Food Sci. Food Saf.*, 2021, **20**, 1887–1909.
- 36 X. Zhang, M. Zhu, Y. Jiang, X. Wang, Z. Guo, J. Shi, X. Zou and E. Han, *J. Hazard. Mater.*, 2020, **400**, 123222.
- 37 L. Zheng, Q. Li, Y. Wu, L. Su, W. Du, J. Song, L. Chen and H. Yang, *Chem. Sci.*, 2023, **14**, 13860–13869.
- 38 M. Zareef, M. Mehedi Hassan, M. Arslan, W. Ahmad, S. Ali, Q. Ouyang, H. Li, X. Wu and Q. Chen, *Microchem. J.*, 2020, **159**, 105431.
- 39 L. Jiang, M. M. Hassan, S. Ali, H. Li, R. Sheng and Q. Chen, *Trends Food Sci. Technol.*, 2021, **112**, 225–240.
- 40 J. Zhai, X. Li, J. Zhang, H. Pan, Q. Peng, H. Gan, S. Su, L. Yuwen and C. Song, *Sens. Actuators, B*, 2022, **368**, 132245.
- 41 R. Sun, Y. Li, T. Du and Y. Qi, *Trends Food Sci. Technol.*, 2023, **135**, 14–31.
- 42 N. Duan, Y. Chang, T. Su, X. Zhang, M. Lu, Z. Wang and S. Wu, *Biosens. Bioelectron.*, 2024, **249**, 116022.
- 43 J. Chen, C. Zhang, L. Yi, F. Duan, Y. Gu, K. Ge and X. Fan, *Food Chem.:X*, 2024, **24**, 101958.
- 44 L. Fang, M. Jia, H. Zhao, L. Kang, L. Shi, L. Zhou and W. Kong, *Trends Food Sci. Technol.*, 2021, **116**, 387–404.
- 45 D. A. Long, *Raman Spectrosc.*, 2001, **34**, 180.
- 46 L. Maia, V. Oliveira, H. Edwards and L. F. De Oliveira, *ChemPhysChem*, 2021, **22**, 231.
- 47 S. Cong, X. Liu, Y. Jiang, W. Zhang and Z. Zhao, *The Innovation*, 2020, **1**, 100051.
- 48 H. Li, Q. Chen, M. Mehedi Hassan, X. Chen, Q. Ouyang, Z. Guo and J. Zhao, *Biosens. Bioelectron.*, 2017, **92**, 192–199.
- 49 D. Zhang, H. Pu, L. Huang and D.-W. Sun, *Trends Food Sci. Technol.*, 2021, **109**, 690–701.
- 50 L. Ouyang, W. Ren, L. Zhu and J. Irudayaraj, *Rev. Anal. Chem.*, 2017, **36**(1), 20160027.
- 51 T. Li, X. Fan, M. Cai, Y. Jiang, Y. Wang, P. He, J. Ni, A. Mo, C. Peng and J. Liu, *Sci. Total Environ.*, 2023, **905**, 167167.
- 52 R. Peng, T. Zhang, S. Wang, Z. Liu, P. Pan, X. Xu, Y. Song, X. Liu, S. Yan and J. Wang, *Anal. Chem.*, 2024, **96**, 10620–10629.
- 53 J. Guo, F. Zeng, J. Guo and X. Ma, *J. Mater. Sci. Technol.*, 2020, **37**, 96–103.
- 54 X. Tang, Q. Hao, X. Hou, L. Lan, M. Li, L. Yao, X. Zhao, Z. Ni, X. Fan and T. Qiu, *Adv. Mater.*, 2024, **36**, e2312348.
- 55 C. Serafinelli, A. Fantoni, E. Alegria and M. Vieira, *Biosensors*, 2022, **12**, 225.
- 56 X. Bi, D. M. Czajkowsky, Z. Shao and J. Ye, *Nature*, 2024, **628**, 771–775.
- 57 X. Gao, X. Wang, Z. Yang, Y. Shen and A. Xie, *Appl. Surf. Sci.*, 2019, **475**, 135–142.
- 58 Y. Zhou, S. Wang, Y. Yu and X. Teng, *Appl. Surf. Sci.*, 2024, **661**, 160071.
- 59 W. Maneerprakorn, S. Bamrungsap, C. Apiwat and N. Wiriyachaiporn, *RSC Adv.*, 2016, **6**, 112079–112085.
- 60 L. Yang, Y. Peng, Y. Yang, J. Liu, H. Huang, B. Yu, J. Zhao, Y. Lu, Z. Huang, Z. Li and J. R. Lombardi, *Advanced Science*, 2019, **6**, 1900310.
- 61 H. Zhang, Y. Tang, W. Wang, D. Yu, L. Yang, X. Jiang, W. Song and B. Zhao, *Food Chem.*, 2024, **431**, 137163.
- 62 J. Zheng, J. Yan, X. Qi, X. Zhang, Y. Li and M. Zou, *Spectrochim. Acta, Part A*, 2021, **251**, 119396.
- 63 A. Garg, W. Nam and W. Zhou, *ACS Appl. Mater. Interfaces*, 2020, **12**, 56290–56299.
- 64 Q.-K. Fan, T.-Z. Liu, H.-S. Li, S.-M. Zhang, K. Liu and C.-B. Gao, *Rare Met.*, 2020, **39**, 834–840.
- 65 M. Lafuente, S. Ruiz-Rincón, R. Mallada, P. Cea and M. Pilar Pina, *Appl. Surf. Sci.*, 2020, **506**, 144663.
- 66 M. Celik, S. Altuntas and F. Buyukserin, *Sens. Actuators, B*, 2018, **255**, 2871–2877.
- 67 B. Lin, Y. Yao, Y. Wang, P. Kannan, L. Chen and L. Guo, *Analyst*, 2021, **146**, 7168–7177.
- 68 L. Liang, X. Zhao, J. Wen, J. Liu, F. Zhang, X. Guo, K. Zhang, A. Wang, R. Gao and Y. Wang, *Langmuir*, 2022, **38**, 13753–13762.
- 69 C. Zhang, L. Huang, H. Pu and D.-W. Sun, *Trends Food Sci. Technol.*, 2021, **113**, 366–381.
- 70 L. Liu, D. Li and W. Deng, *Biosens. Bioelectron.*, 2021, **180**, 113138.
- 71 D. Xia, P. Jiang, Z. Cai, R. Zhou, B. Tu, N. Gao, G. Chang, H. He and Y. He, *Microchim. Acta*, 2022, **189**, 232.
- 72 Z. Zhou, X. Bai, P. Li, C. Wang, M. Guo, Y. Zhang, P. Ding, S. Chen, Y. Wu and Q. Wang, *Chin. Chem. Lett.*, 2021, **32**, 1497–1501.
- 73 Q. Wang, Y. Liu, Y. Bai, S. Yao, Z. Wei, M. Zhang, L. Wang and L. Wang, *Anal. Chim. Acta*, 2019, **1049**, 170–178.
- 74 L. Yao, P. Dai, L. Ouyang and L. Zhu, *Microchem. J.*, 2021, **160**, 105728.
- 75 J. Yang, J. Xu, X. Bian, Y. Pu, K. L. Chiu, D. Miao and S. Jiang, *Cellulose*, 2021, **28**, 921–936.
- 76 M. S. S. Bharati and V. R. Soma, *Opto-Electron. Adv.*, 2021, **4**, 210048.
- 77 Y. Hu, Y. Zhou, G. Luo, D. Li and M. Qu, *Int. J. Extreme Manuf.*, 2024, **6**, 045005.
- 78 T. K. Naqvi, A. K. Srivastava, M. M. Kulkarni, A. M. Siddiqui and P. K. Dwivedi, *Appl. Surf. Sci.*, 2019, **478**, 887–895.
- 79 L. Vázquez-Iglesias, G. M. S. Casagrande, D. García-Lojo, L. F. Leal, T. A. Ngo, J. Pérez-Juste, R. M. Reis, K. Kant and I. Pastoriza-Santos, *Bioact. Mater.*, 2024, **34**, 248–268.
- 80 R. Gao, F. Chen, D. Yang, L. Zheng, T. Jing, H. Jia, X. Chen, Y. Lu, S. Xu and D. Zhang, *Sens. Actuators, B*, 2022, **369**, 132378.

- 81 Y. Chen, Z. Zhang, Y. Wu, Y. Wu, J. Wang, M. Liu and L. Chen, *Langmuir*, 2024, **40**, 21832–21841.
- 82 Z. Zhang, Y. Wu, X. Cao, J. Gao, S. Yan, S. Su, Y. Wu, N. Zhou, X. Wang and L. Chen, *Nano Lett.*, 2024, **24**, 15127–15135.
- 83 Y.-W. Cheng, C.-W. Hsiao, Z.-L. Zeng, W.-L. Syu and T.-Y. Liu, *Surf. Coat. Technol.*, 2020, **389**, 125653.
- 84 R. Gao, H. Qian, C. Weng, X. Wang, C. Xie, K. Guo, S. Zhang, S. Xuan, Z. Guo and L.-B. Luo, *Sens. Actuators, B*, 2020, **321**, 128543.
- 85 K. Wang, D.-W. Sun, H. Pu, Q. Wei and L. Huang, *ACS Appl. Mater. Interfaces*, 2019, **11**, 29177–29186.
- 86 X. Bian, J. Xu, Y. Pu, J. Yang, K.-I. Chiu and S. Jiang, *J. Ind. Text.*, 2022, **51**, 712S–727S.
- 87 K. V. Serebrennikova, A. N. Berlina, D. V. Sotnikov, A. V. Zherdev and B. B. Dzantiev, *Biosensors*, 2021, **11**(12), 512.
- 88 Y. Zhao, L. Shi, H. Miao and X. Jing, *Anal. Chem.*, 2021, **93**(6), 3250–3257.
- 89 W. Tong, G. Tao, Y. Wu, X. Chen, Y. Leng, X. Huang and Y. Xiong, *Trends Food Sci. Technol.*, 2023, **142**, 104243.
- 90 B. Lin, P. Kannan, B. Qiu, Z. Lin and L. Guo, *Food Chem.*, 2020, **307**, 125528.
- 91 S. Zheng, C. Wang, J. Li, W. Wang, Q. Yu, C. Wang and S. Wang, *Chem. Eng. J.*, 2022, **448**, 137760.
- 92 S. Chakraborty, V. Awasthi, R. Goel and S. K. Dubey, *Opt. Mater.*, 2024, **154**, 115647.
- 93 Y.-H. Chen, C.-C. Chen, L.-C. Lu, C.-Y. Lan, H.-L. Chen, T.-H. Yen and D. Wan, *Sens. Actuators, B*, 2023, **391**, 134035.
- 94 Y. Wang, K. Jia and J. Lin, *TrAC, Trends Anal. Chem.*, 2024, **177**, 117785.
- 95 Y. Wang, B. Yan and L. Chen, *Chem. Rev.*, 2013, **113**, 1391–1428.
- 96 H. Li, S. A. Haruna, W. Sheng, Q. Bei, W. Ahmad, M. Zareef, Q. Chen and Z. Ding, *TrAC, Trends Anal. Chem.*, 2023, **169**, 117365.
- 97 Z. Wu, D.-W. Sun, H. Pu, Q. Wei and X. Lin, *Food Chem.*, 2022, **372**, 131293.
- 98 P. She, Y. Chu, C. Liu, X. Guo, K. Zhao, J. Li, H. Du, X. Zhang, H. Wang and A. Deng, *Anal. Chim. Acta*, 2016, **906**, 139–147.
- 99 R. Chen, Y. Sun, B. Huo, Z. Mao, X. Wang, S. Li, R. Lu, S. Li, J. Liang and Z. Gao, *Anal. Chim. Acta*, 2021, **1180**, 338888.
- 100 H. Li, Y. Wang, Y. Li, J. Zhang, Y. Qiao, Q. Wang and G. Che, *J. Phys. Chem. Solids*, 2020, **138**, 109254.
- 101 N. Duan, B. Chang, H. Zhang, Z. Wang and S. Wu, *Int. J. Food Microbiol.*, 2016, **218**, 38–43.
- 102 H. H. Li, Q. S. Chen, Q. Ouyang and J. W. Zhao, *Food Anal. Methods*, 2017, **10**, 3032–3041.
- 103 S. Chattopadhyay, P. K. Sabharwal, S. Jain, A. Kaur and H. Singh, *Anal. Chim. Acta*, 2019, **1067**, 98–106.
- 104 N. Duan, Y. Yan, S. Wu and Z. Wang, *Food Control*, 2016, **63**, 122–127.
- 105 S. Wu, L. Liu, N. Duan, Q. Li, Y. Zhou and Z. Wang, *J. Agric. Food Chem.*, 2018, **66**, 1949–1954.
- 106 N. Duan, M. Shen, S. Qi, W. Wang, S. Wu and Z. Wang, *Spectrochim. Acta, Part A*, 2020, **230**, 118103.
- 107 Y. Sun, N. Zhang, C. Han, Z. Chen, X. Zhai, Z. Li, K. Zheng, J. Zhu, X. Wang, X. Zou, X. Huang and J. Shi, *Food Chem.*, 2021, **358**, 129898.
- 108 B. Xie, Z.-P. Wang, R. Zhang, Z. Zhang and Y. He, *Anal. Chim. Acta*, 2022, **1190**, 339175.
- 109 Y.-W. Weng, X.-D. Hu, L. Jiang, Q.-L. Shi and X.-L. Wei, *Anal. Bioanal. Chem.*, 2021, **413**, 5419–5426.
- 110 X. Ma, X. Lin, X. Xu and Z. Wang, *Microchim. Acta*, 2021, **188**, 202.
- 111 X. Zhu, Y. Ning, Z. Zhang, Y. Wen, Y. Zhao and H. Wang, *Anal. Bioanal. Chem.*, 2023, **415**, 1529–1543.
- 112 X. Zhu, Y. Zhao, Z. Zhang, H. Wang, B. Liu, Z. Li and M. Wang, *Microchim. Acta*, 2021, **188**, 396.
- 113 K. M. Nunes, M. V. O. Andrade, A. M. P. Santos Filho, M. C. Lasmar and M. M. Sena, *Food Chem.*, 2016, **205**, 14–22.
- 114 Z. M. Guo, P. Chen, N. Yosri, Q. S. Chen, H. R. Elseedi, X. B. Zou and H. S. Yang, *Food Rev. Int.*, 2023, **39**, 1440–1461.
- 115 J. J. Wang, Q. S. Chen, T. Belwal, X. Y. Lin and Z. S. Luo, *Compr. Rev. Food Sci. Food Saf.*, 2021, **20**, 2476–2507.
- 116 J. J. Zhu, A. A. Agyekum, F. Y. H. Kutsanedzie, H. H. Li, Q. S. Chen, Q. Ouyang and H. Jiang, *LWT-Food Sci. Technol.*, 2018, **97**, 760–769.
- 117 H. Li, M. Mehedi Hassan, J. Wang, W. Wei, M. Zou, Q. Ouyang and Q. Chen, *Food Chem.*, 2021, **339**, 127843.
- 118 Z. Guo, M. Wang, A. O. Barimah, Q. Chen, H. Li, J. Shi, H. R. El-Seedi and X. Zou, *Int. J. Food Microbiol.*, 2021, **338**, 108990.
- 119 S. Liu, H. Li, M. M. Hassan, J. Zhu, A. Wang, Q. Ouyang, M. Zareef and Q. Chen, *Int. J. Food Microbiol.*, 2019, **304**, 58–67.
- 120 S. Y.-S. S. Adade, H. Lin, N. A. N. Johnson, S. Qianqian, X. Nunekpeku, W. Ahmad, B. A. Kwadzokpui, J.-N. Ekumah and Q. Chen, *Food Chem.*, 2024, **454**, 139836.
- 121 H. Jiang, Y. C. He, W. D. Xu and Q. S. Chen, *Food Anal. Methods*, 2021, **14**, 1826–1835.
- 122 Z. Guo, P. Chen, L. Yin, M. Zuo, Q. Chen, H. R. El-Seedi and X. Zou, *Food Control*, 2022, **132**, 108498.
- 123 T. Jiao, M. Mehedi Hassan, J. Zhu, S. Ali, W. Ahmad, J. Wang, C. Lv, Q. Chen and H. Li, *Food Chem.*, 2021, **337**, 127652.
- 124 P. Zeng, Q. Guan, Q. Zhang, L. Yu, X. Yan, Y. Hong, L. Duan and C. Wang, *Microchim. Acta*, 2023, **191**, 28.
- 125 Z. Guo, M. Wang, J. Wu, F. Tao, Q. Chen, Q. Wang, Q. Ouyang, J. Shi and X. Zou, *Food Chem.*, 2019, **286**, 282–288.
- 126 X. Zhang, Z. Wang, X. Huang, Q. Huang, Y. Wen, B. Li, M. Holmes, J. Shi and X. Zou, *Chem. Eng. J.*, 2023, **451**, 138928.
- 127 X. Zhang, Y. Zhou, X. Huang, X. Hu, X. Huang, L. Yin, Q. Huang, Y. Wen, B. Li, J. Shi and X. Zou, *Food Chem.*, 2023, **407**, 135115.
- 128 M. Wang, F. Shi, J. Li, L. Min, Z. Yang and J. Li, *Chem. Commun.*, 2024, **60**, 6019–6022.
- 129 C. Song, J. Li, Y. Sun, X. Jiang, J. Zhang, C. Dong and L. Wang, *Sens. Actuators, B*, 2020, **310**, 127849.

- 130 J. Dai, J. Li, Y. Jiao, X. Yang, D. Yang, Z. Zhong, H. Li and Y. Yang, *Food Chem.*, 2024, **456**, 139955.
- 131 T. Wu, J. Li, S. Zheng, Q. Yu, K. Qi, Y. Shao, C. Wang, J. Tu and R. Xiao, *Biosensors*, 2022, **12**(9), 709.
- 132 R. Zhang, S. Xie, X. Yang, Y. Tang, J. Liu, M. Liao, M. Wang and Y. He, *Microchim. Acta*, 2025, **192**, 62.
- 133 Y. Zhao, M. Guan, F. Mi, Y. Zhang, P. Geng, S. Zhang, H. Song and G. Chen, *Microchim. Acta*, 2025, **192**, 83.
- 134 L. Wu, Y. Li, Y. Han, X. Liu, B. Han, H. Mao and Q. Chen, *J. Food Compos. Anal.*, 2024, **130**, 106190.
- 135 M. Zhang and X. Guo, *Trends Food Sci. Technol.*, 2022, **129**, 621–633.
- 136 C. Zhang, Y. Han, L. Lin, N. Deng, B. Chen and Y. Liu, *J. Agric. Food Chem.*, 2017, **65**, 1290–1295.
- 137 L. Xue, L. Zheng, H. Zhang, X. Jin and J. Lin, *Sens. Actuators, B*, 2018, **265**, 318–325.
- 138 N. Duan, W. Sun, S. Wu, L. Liu, X. Hun and Z. Wang, *Sens. Actuators, B*, 2018, **255**, 2582–2588.
- 139 Y. Rong, S. Ali, Q. Ouyang, L. Wang, H. Li and Q. Chen, *J. Food Compos. Anal.*, 2021, **100**, 103929.
- 140 X. Gao, Y. Liu, J. Wei, Z. Wang and X. Ma, *Spectrochim. Acta, Part A*, 2024, **315**, 124268.
- 141 C. Sun, W. Dong, J. Peng, X. Wan, Z. Sun, D. Li and S. Wang, *Sens. Actuators, B*, 2020, **325**, 128644.
- 142 J. Qi, J. Li, Y. Wan, Y. Li and F. Pi, *Food Chem.*, 2024, **435**, 137586.
- 143 J. Baranwal, B. Barse, G. Gatto, G. Broncova and A. Kumar, *Chemosensors*, 2022, **10**(9), 363.
- 144 J. Lopez-Tellez, S. Ramirez-Montes, T. A. Ferreira, E. M. Santos and J. A. Rodriguez, *Chemosensors*, 2022, **10**(10), 424.
- 145 D. A. Aikens, *J. Chem. Educ.*, 1983, **60**, A25.
- 146 A. Lazanas and M. Prodromidis, *ACS Meas. Sci. Au*, 2023, **3**(3), 162–193.
- 147 H. Chen, J. Wang, W. Zhang, Y. Li, X. Zhang, X. Huang, Y. Shi, Y. Zou, Z. Li, J. Shi and X. Zou, *J. Food Compos. Anal.*, 2025, **140**, 107266.
- 148 Y. Zeng, Z. Zhu, D. Du and Y. Lin, *J. Electroanal. Chem.*, 2016, **781**, 147–154.
- 149 W. Lu, X. Dai, R. Yang, Z. Liu, H. Chen, Y. Zhang and X. Zhang, *Food Control*, 2025, **169**, 111006.
- 150 X. Zhang, Y. Zhou, J. Wang, X. Huang, H. S. El-Mesery, Y. Shi, Y. Zou, Z. Li, Y. Li, J. Shi and X. Zou, *Food Chem.*, 2025, **467**, 142342.
- 151 X. Zhang, Y. Zhou, H. Wang, X. Huang, Y. Shi, Y. Zou, X. Hu, Z. Li, J. Shi and X. Zou, *Anal. Chim. Acta*, 2024, **1304**, 342515.
- 152 S. Cheng, Y. Hou, X. Wen, D. Xu, X. Luo and H. Cao, *Sens. Actuators, B*, 2025, **422**, 136601.
- 153 T. Lin, Y. Xu, A. Zhao, W. He and F. Xiao, *Anal. Chim. Acta*, 2022, **1207**, 339461.
- 154 F. Zahirifar, M. Rahimnejad, R. A. Abdulkareem and G. Najafpour, *Biocatal. Agric. Biotechnol.*, 2019, **20**, 101245.
- 155 X. Wang, Y. Xu, Y. Li, Y. Li, Z. Li, W. Zhang, X. Zou, J. Shi, X. Huang, C. Liu and W. Li, *Food Chem.*, 2021, **357**, 129762.
- 156 G. Qin, Y. Kong, T. Gan and Y. Ni, *Inorg. Chem.*, 2022, **61**, 8966–8975.
- 157 K. Prabhu, S. J. Malode, R. M. Kulkarni and N. P. Shetti, *New J. Chem.*, 2023, **47**, 315–323.
- 158 W. Li, P. Wang, B. Chu, X. Chen, Z. Peng, J. Chu, R. Lin, Q. Gu, J. Lu and D. Wu, *Food Chem.*, 2023, **402**, 134197.
- 159 X. Zhang, X. Huang, Y. Xu, X. Wang, Z. Guo, X. Huang, Z. Li, J. Shi and X. Zou, *Biosens. Bioelectron.*, 2020, **168**, 112544.
- 160 X. A. Zhang, C. Y. Huang, Y. J. Jiang, Y. X. Jiang, J. Z. Shen and E. Han, *J. Agric. Food Chem.*, 2018, **66**, 10106–10112.
- 161 C. Liu, Y. Y. Li, T. Chen, S. Y. Meng, D. Liu, D. M. Dong and T. Y. You, *J. Agric. Food Chem.*, 2022, **70**, 7412–7419.
- 162 C. Zhu, D. Liu, Y. Li, T. Chen and T. You, *Food Chem.*, 2022, **373**, 131443.
- 163 X. Huang, C. Huang, L. Zhou, G. Hou, J. Sun, X. Zhang and X. Zou, *Anal. Chim. Acta*, 2023, **1278**, 341752.
- 164 S. Liu, S. Meng, M. Wang, W. Li, N. Dong, D. Liu, Y. Li and T. You, *Food Chem.*, 2023, **410**, 135450.
- 165 Y. Y. Li, S. Y. Meng, N. Dong, Y. Wei, Y. Wang, X. Li, D. Liu and T. Y. You, *J. Agric. Food Chem.*, 2023, **71**, 14806–14813.
- 166 P. Murasova, A. Kovarova, J. Kasparova, I. Brozkova, A. Hamiot, J. Pekarkova, B. Dupuy, J. Drbohlavova, Z. Bilkova and L. Korecka, *J. Electroanal. Chem.*, 2020, **863**, 114051.
- 167 L. Zhu, X.-X. Dong, C.-B. Gao, Z. Gai, Y.-X. He, Z.-J. Qian, Y. Liu, H.-T. Lei, Y.-M. Sun and Z.-L. Xu, *Food Control*, 2022, **133**, 108662.
- 168 E. Han, M. Zhang, Y. Pan and J. Cai, *Materials*, 2022, **15**(8), 2809.
- 169 X. Tang, T. Wu, F. Pan, G. Lu, W. Zeng, W. Fan and L. Wu, *Sens. Actuators, B*, 2024, **404**, 135279.
- 170 T. Wu, X. Tang, W. Zeng, Y. Han, S. Zhang, J. Wei and L. Wu, *J. Food Eng.*, 2024, **378**, 112109.
- 171 X. Tang, R. Wen, C. Ji, J. Wei, Y. Han and L. Wu, *Microchem. J.*, 2024, **206**, 111524.
- 172 A. Ostovan, M. Arabi, Y. Wang, J. Li, B. Li, X. Wang and L. Chen, *Adv. Mater.*, 2022, **34**, 2203154.
- 173 M. Arabi, A. Ostovan, Y. Wang, R. Mei, L. Fu, J. Li, X. Wang and L. Chen, *Nat. Commun.*, 2022, **13**, 5757.
- 174 N. Wang, R. Hong, G. Zhang, M. Pan, Y. Bao and W. Zhang, *Small*, 2024, 2409078.
- 175 M. Arabi and L. Chen, *Langmuir*, 2022, **38**, 5963–5967.
- 176 C. Zhang, X. Shi, F. Yu and Y. Quan, *Food Chem.*, 2020, **317**, 126431.
- 177 Z. Dong, J. Lu, Y. Wu, M. Meng, C. Yu, C. Sun, M. Chen, Z. Da and Y. Yan, *Food Chem.*, 2020, **333**, 127477.
- 178 X. Su, K. Zheng, X. Tian, X. Zhou, X. Zou, X. Xu, Z. Sun and W. Zhang, *Food Chem.*, 2023, **429**, 136927.
- 179 W. M. Yang, C. H. Liu, B. L. Zhang, C. C. Wu, Y. Cao, W. H. Huang and W. Z. Xu, *Food Anal. Methods*, 2024, **17**, 1689–1701.
- 180 C. C. Qin, W. L. Guo, Y. Liu, Z. C. Liu, J. Qiu and J. B. Peng, *Food Anal. Methods*, 2017, **10**, 2293–2301.
- 181 E. Han, Y. Pan, L. Li and J. Cai, *Food Chem.*, 2023, **426**, 136608.
- 182 G. Liu, Z. Chen, X. Jiang, D.-Q. Feng, J. Zhao, D. Fan and W. Wang, *Sens. Actuators, B*, 2016, **228**, 302–307.
- 183 C. Li, Q. Yang, X. Wang, M. Arabi, H. Peng, J. Li, H. Xiong and L. Chen, *Food Chem.*, 2020, **319**, 126575.

- 184 H. Qiu, L. Gao, J. Wang, J. Pan, Y. Yan and X. Zhang, *Food Chem.*, 2017, **217**, 620–627.
- 185 Z. Zhou, T. Li, W. Xu, W. Huang, N. Wang and W. Yang, *Sens. Actuators, B*, 2017, **240**, 1114–1122.
- 186 Y. Xu, T. Huang, S. Wang and Y. Yan, *J. Food Compos. Anal.*, 2022, **108**, 104427.
- 187 H. Lu and S. Xu, *Sens. Actuators, B*, 2020, **306**, 127566.
- 188 J. Li, J. Cheng, J. Du, M. Xiao, M. Wang, J. Wang, Y. She, A. M. Abd El-Aty and X. Cao, *J. Food Compos. Anal.*, 2024, **133**, 106380.
- 189 J. Ju, S. Cong, Y. Hu, Z. Xu, Z. Ji, R. Xu, Z. Zhang and X. Cao, *J. Food Compos. Anal.*, 2025, **139**, 107170.
- 190 H. Guo, H. Li, M. Xu, J. Zhou, D. Zhang, D. Wang and W. Sun, *Spectrochim. Acta, Part A*, 2025, **327**, 125393.
- 191 M. Hui, X. Ma, J. Yuan, Z. Wang and X. Ma, *Anal. Bioanal. Chem.*, 2025, **417**, 1127–1138.
- 192 D. Kim, J. Kim, J. Henzie, Y. Ko, H. Lim, G. Kwon, J. Na, H.-J. Kim, Y. Yamauchi and J. You, *Chem. Eng. J.*, 2021, **419**, 129445.
- 193 T. Xie, Z. Cao, Y. Li, Z. Li, F.-L. Zhang, Y. Gu, C. Han, G. Yang and L. Qu, *Food Chem.*, 2022, **381**, 132208.
- 194 X. Chen, A. Ostovan, M. Arabi, Y. Wang, L. Chen and J. Li, *Anal. Chem.*, 2024, **96**, 6417–6425.
- 195 M. Arabi, A. Ostovan, Z. Zhang, Y. Wang, R. Mei, L. Fu, X. Wang, J. Ma and L. Chen, *Biosens. Bioelectron.*, 2021, **174**, 112825.
- 196 Y. Xu, W. Huang, H. Duan and F. Xiao, *Biosens. Bioelectron.*, 2024, **260**, 116463.
- 197 S. Yan, F. Chu, H. Zhang, Y. Yuan, Y. Huang, A. Liu, S. Wang, W. Li, S. Li and W. Wen, *Spectrochim. Acta, Part A*, 2019, **220**, 117113.
- 198 Y. Gong, D. Li, M. Chen, A. Lin, Q. Chen and X. Chen, *Anal. Chim. Acta*, 2025, **1335**, 343471.
- 199 G. Emonds-Alt, C. Malherbe, A. Kasemiire, H. T. Avohou, P. Hubert, E. Ziemons, J.-C. M. Monbaliu and G. Eppe, *Talanta*, 2022, **249**, 123640.
- 200 R. Deng, L. Xu, Y. Zhang, X. Zhang, Z. Yuan, J. Chen and X. Xia, *Trends Food Sci. Technol.*, 2024, **145**, 104351.
- 201 J. Zhuang, Z. Zhao, K. Lian, L. Yin, J. Wang, S. Man, G. Liu and L. Ma, *Biosens. Bioelectron.*, 2022, **207**, 114167.
- 202 L. Zhang, R. Huang, W. Liu, H. Liu, X. Zhou and D. Xing, *Biosens. Bioelectron.*, 2016, **86**, 1–7.
- 203 L. Meiqing, L. Jinyang, M. Hanping and W. Yanyou, *Biosyst. Eng.*, 2016, **143**, 108–118.
- 204 J. Sun, Y. H. Liu, G. S. Wu, Y. C. Zhang, R. B. Zhang and X. J. Li, *J. Food Qual.*, 2021, 2021.
- 205 X. D. Zhai, Z. H. Li, J. J. Zhang, J. Y. Shi, X. Y. Zou, X. W. Huang, D. Zhang, Y. Sun, Z. K. Yang, M. Holmes, Y. Y. Gong and M. Povey, *J. Agric. Food Chem.*, 2018, **66**, 12836–12846.
- 206 Z. Yang, X. Zhai, X. Zou, J. Shi, X. Huang, Z. Li, Y. Gong, M. Holmes, M. Povey and J. Xiao, *Food Chem.*, 2021, **336**, 127634.
- 207 Z. Yang, X. Zhai, C. Zhang, J. Shi, X. Huang, Z. Li, X. Zou, Y. Gong, M. Holmes, M. Povey and J. Xiao, *Food Hydrocolloids*, 2022, **123**, 107187.
- 208 Y. Xin, Z. Wang, H. Yao, W. Liu, Y. Miao, Z. Zhang and D. Wu, *Sens. Actuators, B*, 2023, **393**, 134285.
- 209 B. Wang, C.-Y. Wei, K.-W. Wang, B. Fu, Y. Chen, Y. Han and Z. Zhang, *Biosens. Bioelectron.*, 2023, **239**, 115601.
- 210 L. Luo, X. Liu, S. Ma, L. Li and T. You, *Food Chem.*, 2020, **322**, 126778.
- 211 X. Du, W. Du, J. Sun and D. Jiang, *Food Chem.*, 2022, **385**, 132731.
- 212 S. Y. Meng, D. Liu, Y. Y. Li, N. Dong, T. Chen and T. Y. You, *J. Agric. Food Chem.*, 2022, **70**, 13583–13591.
- 213 C. Q. Wang, X. Zhao, C. D. Gu, F. Y. Xu, W. H. Zhang, X. Y. Huang and J. Qian, *Food Anal. Methods*, 2022, **15**, 3390–3399.
- 214 J. Lai, L. Ding, Y. Liu, C. Fan, F. You, J. Wei, J. Qian and K. Wang, *Food Chem.*, 2023, **423**, 136285.
- 215 X. Zhang, Z. Wang, X. Huang, X. Hu, Y. Li, Y. Zhou, X. Wang, R. Zhang, X. Wei, X. Zhai, J. Zhang, Z. Li, Y. Zhang, Y. Zou, Y. Shi, T. Shen, J. Sun, S. Kang, J. Shi and X. Zou, *Adv. Funct. Mater.*, 2024, **34**, 2312053.
- 216 H. Xiao-wei, L. Zhi-hua, Z. Xiao-bo, S. Ji-yong, M. Han-ping, Z. Jie-wen, H. Li-min and M. Holmes, *Food Chem.*, 2016, **197**, 930–936.
- 217 S. Park, K. Kim, A. Go, M.-H. Lee, L. Chen and J. Choo, *ACS Sens.*, 2025, **10**, 1217–1227.
- 218 J. S. Gootenberg, O. O. Abudayyeh, J. W. Lee, P. Essletzbichler, A. J. Dy, J. Joung, V. Verdine, N. Donghia, N. M. Daringer and C. A. Freije, *Science*, 2017, **356**, 438–442.
- 219 A. Özcan, R. Krajcski, E. Ioannidi, B. Lee, A. Gardner, K. S. Makarova, E. V. Koonin, O. O. Abudayyeh and J. S. Gootenberg, *Nature*, 2021, **597**, 720–725.
- 220 H. Kim, S. Lee, H. W. Seo, B. Kang, J. Moon, K. G. Lee, D. Yong, H. Kang, J. Jung, E.-K. Lim, J. Jeong, H. G. Park, C.-M. Ryu and T. Kang, *ACS Nano*, 2020, **14**, 17241–17253.
- 221 Q. Xiong, C. Y. Lim, J. Ren, J. Zhou, K. Pu, M. B. Chan-Park, H. Mao, Y. C. Lam and H. Duan, *Nat. Commun.*, 2018, **9**, 1743.
- 222 M. Kim, S. Huh, H. J. Park, S. H. Cho, M.-Y. Lee, S. Jo and Y. S. Jung, *Biosens. Bioelectron.*, 2024, **251**, 116128.
- 223 D. Akinwande and D. Kireev, *Nature*, 2019, **576**, 220–221.
- 224 R. Paul, E. Ostermann, Y. Chen, A. C. Saville, Y. Yang, Z. Gu, A. E. Whitfield, J. B. Ristaino and Q. Wei, *Biosens. Bioelectron.*, 2021, **187**, 113312.
- 225 S. V. Puttaswamy, G. V. Lubarsky, C. Kelsey, X. Zhang, D. Finlay, J. A. McLaughlin and N. Bhalla, *ACS Nano*, 2020, **14**, 11939–11949.
- 226 C. Kolluru, R. Gupta, Q. Jiang, M. Williams, H. Gholami Derami, S. Cao, R. K. Noel, S. Singamaneni and M. R. Prausnitz, *ACS Sens.*, 2019, **4**, 1569–1576.
- 227 X. Yi, Z. Yuan, X. Yu, L. Zheng and C. Wang, *ACS Appl. Mater. Interfaces*, 2023, **15**, 4873–4882.
- 228 E. S. Okeke, T. P. C. Ezeorba, C. O. Okoye, Y. Chen, G. Mao, W. Feng and X. Wu, *J. Food Compos. Anal.*, 2022, **114**, 104778.